Spatial Ecology of Arctic Grayling in the Parsnip Core Area

Fish and Wildlife Compensation Program
Peace Project No. PEA-F22-F-3388

Prepared for:

Fish and Wildlife Compensation Program Peace Region
3333 22nd Ave
Prince George, BC
V2N 1B4

Prepared by:

Eduardo Martins, Bryce O'Connor, Joseph Bottoms, Ian Clevenger, Devon Smith, Marie Auger-Methé, Michael Power, David Patterson, Mark Shrimpton and Steven Cooke

University of Northern British Columbia
3333 University Way
Prince George, BC
V2N 4Z9

Prepared with financial support of the Fish and Wildlife Compensation Program on behalf of its program partners BC Hydro, the Province of BC, Fisheries and Oceans Canada, First Nations and Public Stakeholders.

04-July-2022

Executive Summary

Flooding of the Upper Peace basin after construction of the W.A.C. Bennett Dam in 1967 resulted in a considerable loss of riverine habitat to Arctic Grayling (*Thymallus arcticus*). The decrease in riverine habitat, alteration of natural hydrology and drastic reductions in abundance caused great concern for the sustainability of Arctic Grayling populations in the Williston Reservoir Watershed. The recent review by Stamford et al. (2017) and monitoring framework by Hagen and Stamford (2017) highlighted a number of critical information gaps related to the spatial ecology of Arctic Grayling such as: (1) the unknown distribution of Arctic Grayling within the streams of the different core areas (*sensu* Stamford et al. 2017); and (2) the lack of understanding of Arctic Grayling migrations. Furthermore, it is unknown whether populations of Bull Trout (*Salvelinus confluentus*) are limiting the abundance of Arctic Grayling and their spatial distribution.

The goal of this project is to investigate the spatial ecology (seasonal migrations and spatial distribution) of sub-adult and adult Arctic Grayling and their interactions with Bull Trout in the Parsnip River mainstem and tributaries, a core area of Arctic Grayling populations in the Williston Reservoir Watershed.

The information gathered in this study will fill in data gaps that were identified as moderate and high immediacy for the Parsnip core area (data gaps 5.1.3a-i in Table 6 of Stamford et al. 2017) and will also be relevant to other core areas in the Williston Reservoir Watershed (2.3.1b-c and 2.3.5 in Table 1 of Stamford et al. 2017). Therefore, the outcomes of this study will primarily address the priority action # 9 (PEA.RLR.S03.RI.09) of the *Peace Region Rivers, Lakes, and Reservoirs Action Plan* (FWCP 2020a). However, given that the study will collect data on Bull Trout, it will also contribute information to address priority # 13 (PEA.RLR.S04.RI.13) of the *Peace Region Rivers, Lakes, and Reservoirs Action Plan* (FWCP 2020a), particularly by filling in high immediacy data gaps 5.1a and 5.1b outlined in Table 5.1c in Hagen and Weber (2019).

This report presents results on project activities in Year 4 of 4 but focuses on integrating data and presenting results obtained since Year 1 (2018 to 2021). The methods used to address the study objectives included: acoustic telemetry, capture-recapture, temperature data logging, stable isotope analysis and spatial modeling.

Over the study period there were 171 air (59) and water (112) temperature logger site locations. In 2021, 14 water temperature data loggers were deployed in the watershed. Nine of these water temperature loggers were deployed with associated air temperature loggers. In the fall of 2021, data from 62 water temperature loggers and 45 air temperature loggers were downloaded. After data imputation, a total of 55 complete water temperature times series in 2019, 48 in 2020 and 37 in 2021 were used to compute water temperature metrics and included in the SSNM.

The mean of the three thermal metrics at water observation sites in 2019 were 10.53ºC (± 1.37ºC) for average weekly average temperature (AWAT), 11.70ºC (± 1.61ºC) for maximum weekly average temperature (MWAT) and 0.06 (± 0.01) for AWCV. The mean of the three thermal metrics at water observation sites in 2020 were 9.26ºC (± 1.84ºC) for AWAT, 12.50ºC (± 2.45ºC) for MWAT and 0.08 (± 0.01) for average weekly coefficient of variation (AWCV). The

mean of the three thermal metrics at water observation sites in 2021 were 11.39ºC (± 2.70ºC) for AWAT, 14.24ºC (±3.63ºC) for MWAT and 0.06 (± 0.01) for AWCV.

Spatial stream network models (SSNM) were fit for the 2019-2021 feeding windows (July 1st – September 15th) AWAT, MWAT, AWCV and daily average temperature response metrics. The SSNMs were used to predict continuous temperatures for the entire watershed and visualize trends in average temperature and temperature variability. Elevational gradients supply cold-water to critical summer habitats in the tributaries on the east side of the Parsnip mainstem. In mid-summer, a clear isotherm shift occurs during warm, dry conditions where these critical, lower elevation summer habitats see chronic increases in temperature. Although short-lived, these events may lead to elevated thermal stress for cold-water adapted species. Predictions were exported for use in a spatial capture recapture (SCR) model.

Over the duration of the study, Arctic Grayling and Bull Trout distributions were monitored by an array of acoustic telemetry receivers. Array deployment began in the summer of 2018 and reached full coverage in 2019. Receivers were deployed in a clustered design for array resiliency against losses. Between each season, a subset of receivers was lost to flood events, shifting gravel bed rivers, mechanical damage, and vandalism. Receivers were replaced or relocated as needed, and discontinuous telemetry data were accommodated during analysis through use of spatial capture-recapture. In the initial 2018 season, 55 receivers were deployed. An additional 26 receivers were deployed in 2019, including eight replacements. A major spring flood event occurred in 2020, which led to the loss of 22 receivers, four of which were replaced near critical array junctions. During the summer of 2021, nine receivers were deployed (six replacements, three new) for the season before the end of the study in the fall.

A total of 157 grayling and 63 Bull Trout were tagged with acoustic transmitters between 2018-2021. Over the duration of this study, the acoustic receiver array recorded 3,375,873 detections of the tagged fish in the Parsnip River watershed. Binned into daily datasets of individual detection histories across the study area, there were 13,069 unique observations which were analyzed using a series of 48 spatial capture-recapture models fitted across both short, bi-weekly windows and longer-term monthly windows. Arctic Grayling in the Parsnip River watershed showed three distinct life phases: 1) an overwintering period spent in the Parsnip River mainstem; 2) a spring spawning migration into the middle reaches of the Anzac, Table, Hominka, and Missinka Rivers; and 3) a summer feeding migration in which they may disperse wide across the watershed in search of suitable feeding habitats. Arctic Grayling were observed showing high fidelity to a single Parsnip River tributary during open-water months, with a subset of the sampled population showing an apparently wider ranging behaviour (showing use of two or more tributaries across years). The SCR model outputs indicated that density of tagged grayling home range centres was correlated to both the distribution of thermal habitat availability and Bull Trout presence (based on tagged individuals). Spatial overlap between Arctic Grayling and Bull Trout was at its lowest during the winter months, and was elevated during the summer months, showing some temporal separation of habitat use in the upper tributaries.

A total of 466 biological samples comprised of adipose fin, fish muscle, invertebrate, plant, and particulate organic matter, were obtained for stable isotope analysis. Bull Trout were found to

occupy a larger dietary niche and higher trophic position than Arctic Grayling. The data indicate that Bull Trout consume a diverse selection of dietary items while Arctic Grayling exhibit more homogeneous dietary preferences among individuals. Small (juvenile and sub-adult) Arctic Grayling likely contribute to Bull Trout (particularly those large enough to not be gape limited to consume Arctic Grayling) diet along with other potential prey fish. Arctic Grayling exhibited no relationship between $\delta^{15}N$ and fork length, whereas Bull Trout $\delta^{15}N$ was positively related to fork length.

The project successfully completed the objectives laid out at the start of the 4-year project. Based on ten findings, we recommend that:

1. Prioritize conservation actions in and around small high elevation tributaries which provide cold-water inputs to downstream critical habitats for Arctic Grayling and provide spawning and rearing habitat for Bull Trout.

2. Immediately prioritize areas for land securement and conservation actions which can preserve thermal habitat within the Parsnip River watershed and reduce the impacts of cumulative stressors

3. Pursue research on thermal habitat patterns at sub-watershed scales which may affect the ability of Arctic Grayling and Bull Trout to thermoregulate. While findings on the watershed scale provide foundation for understanding the spatial ecology of Arctic Grayling, sub-watershed scale thermal habitat will further inform how conservation actions could be designed to preserve cold-water thermal habitat for the species.

4. Align thermal habitat monitoring programs across scales (sub-watershed to basin-wide) to ensure insights at multiple spatial and temporal scales in the Williston Reservoir watershed

5. Integrate critical habitat (including findings of this research) and abundance monitoring programs to investigate habitat covariates which affect the spatial distribution and temporal dynamics of priority species for FWCP

6. Investigate Arctic Grayling genetic diversity in the Parsnip River watershed and determine its influence on movement behaviours and thermal adaptative capacity

7. Coordinate partnerships across multiple organizations (First Nations, Provincial Government, public stakeholders and Academia) which share common goals to enhance information and data sharing to support research and implementation of conservation actions

Table of Contents

List of Tables

List of Figures

1. Introduction

The construction of the 183-m high W.A.C. Bennett Dam in 1967, forming the Williston Reservoir flooded roughly 350 km of the Peace, Finlay, and Parsnip River valleys (Hagen and Stamford 2017). Arctic Grayling (*Thymallus arcticus*) in the Upper Peace watershed show a fluvial life history form (Clarke *et al*. 2007). Therefore, flooding of the Upper Peace resulted in a considerable loss of riverine habitat. Prior to impoundment, Arctic Grayling were widespread and abundant in tributary streams of the Upper Peace (Pearce and Abadzadesahraei 2019). However, presently Arctic Grayling are restricted to just eight of the larger watersheds in the Williston Reservoir watershed (Hagen and Stamford 2017). The decrease in available habitat, alteration of natural hydrology (change from large flowing rivers to reservoir) and evidence of drastic reductions in population size cause great uncertainty about the sustainability of Arctic Grayling populations in the Williston Reservoir Watershed (Stamford and Taylor 2005). The recent review by Stamford et al. (2017) and monitoring framework by Hagen and Stamford (2017) highlighted a number of critical information gaps related to the spatial ecology – the causes and consequences of a species distribution over time and space (Hastings et al. 2011) – of Arctic Grayling. For example, two important spatial ecology data gaps identified in the review are: (1) the unknown distribution of Arctic Grayling within the streams of the different core areas (*sensu* Stamford et al. 2017); and (2) the lack of understanding of Arctic Grayling migrations.

Knowledge of a species' spatial ecology is fundamental to the effective development and implementation of enhancement and conservation programs (Allen and Singh 2016, Ogburn et al. 2017). To identify critical habitats and potential limiting factors (e.g. habitat conditions, human impacts, interspecific interactions), these programs often require detailed information derived from spatial ecology studies describing where, when and why individuals move and are distributed in space (Cooke et al. 2016). Although the description of distribution and migrations is a necessary step in understanding the spatial ecology of Arctic Grayling, it is not sufficient to determine its drivers. Both abiotic and biotic factors play an important role in influencing the spatial ecology of species (Royle et al. 2017). Among abiotic factors, the spatio-temporal availability of thermal habitats is one of the most important drivers of fish distribution and migrations in freshwater environments (Lucas and Baras 2001, Isaak et al. 2010). Despite the general perception that the thermal environment in running freshwater is homogeneous, streams exhibit substantial thermal variability at small (10 to 100 m) and large (> 1,000 m) spatial scales due, for example, to the variability in elevation, riparian vegetation shade and groundwater input along their extension (Kurylyk et al. 2015). Temperature has a strong potential to limit growth and distribution of Arctic Grayling populations, as highlighted by Stamford et al. (2017), and it is known that the occurrence of Arctic Grayling and Bull Trout (*Salvelinus confluentus*) is negatively related to water temperature (Hawkshaw et al. 2014, Isaak et al. 2010). Therefore, a full description of the distribution and migrations of Arctic Grayling in the Williston Reservoir Watershed requires a detailed characterization of the distribution of thermal habitats. Spatial stream network modeling (SSNM) provides high resolution predictions of temperature patterns over large spatial extents and their application to animal occurrence data has become more widespread (Isaak et al. 2014). A novel combination of telemetry detection data and spatial modeling will provide a detailed

characterization of Arctic Grayling thermal ecology and available thermal habitat as well as interactions with Bull Trout (see below).

Understanding diets and dietary relationships of coexisting species is important to determine resource partitioning (Wrona et al. 1981) as overlap in dietary resource use is thought to influence spatial ecology and population trends of coexisting fish (Stamford et al. 2017). Coexisting species often exploit different resource niches, resulting in reduced competition between the species (Millinsky 1982). Further, competition influences diet selection, in which competitive individuals select for higher nutrition food sources resulting in others adopting a generalist diet pattern (Milinsky 1982). Interspecific competition has been defined as "the demand of more than one organism for the same resource of the environment in excess of immediate supply" (Larkin 1956). Therefore, dietary trends can be a viewed as the result of single or compounding factors such as habitat availability, stream productivity, spatial distribution and interspecific competition (Evangelista et al. 2014, Magnan and Fitzgerald 1984). Intraspecific competition can also drive diet preference as larger, dominant individuals establish feeding hierarchies within a species (Hughes 1992). Feeding hierarchies have been observed within freshwater fish populations where larger fish tend to outcompete other individuals for optimal feeding positions (Hughes 1992). In the Williston Reservoir Watershed, Arctic Grayling co-occur with Bull Trout in streams of several core areas, and there is a strong potential for size-dependent overlap in resource use. For example, as juveniles, both species prey heavily on terrestrial drift, aquatic insects and other invertebrate prey and individuals larger than 150 mm will increasingly include fish as prey (Stewart *et al*. 2007a,b). Arctic Grayling feeding behavior also appears to be related to the degree of competition for prey resources (Stewart et al. 2007b). Overlap in resource use and/or risks of predation by larger Bull Trout on smaller Arctic Grayling may significantly influence the spatial ecology of Arctic Grayling in ways that limit the potential growth of its populations (Stamford et al. 2017). Therefore, examining trophic positions of multiple species, trends in dietary niche between Bull Trout and Arctic Grayling, as well as dietary breadths of both species is necessary to characterize the trophic relationships at the community, interspecific and intraspecific levels.

2. Objectives and Linkage to FWCP Action Plans and Priority Actions

The goal of this project is to investigate the spatial ecology of sub-adult and adult Arctic Grayling and their interactions with Bull Trout in the Parsnip mainstem and tributaries, a core area of Arctic Grayling populations in the Williston Reservoir Watershed. Specifically, the objectives are to:

i. Investigate the migrations of sub-adult and adult Arctic Grayling among the Parsnip mainstem, tributaries and a nearby watershed (Pack River);
ii. Describe and define the distribution and thermal habitat use of sub-adult and adult Arctic Grayling;
iii. Determine the overlap in distribution patterns of sub-adult and adult Arctic Grayling and Bull Trout;
iv. Determine the patterns of resource use and the resulting trophic relationship between Arctic Grayling and Bull Trout.

The information gathered in this study will fill in data gaps that were identified as moderate and high immediacy for the Parsnip core area (data gaps 5.1.3a-i in Table 6 of Stamford et al. 2017) and will also be relevant to other core areas in the Williston Reservoir Watershed (2.3.1b-c and 2.3.5 in Table 1 of Stamford et al. 2017). Therefore, the outcomes of this study will primarily address the priority action # 9 (PEA.RLR.S03.RI.09) of the *Peace Region Rivers, Lakes, and Reservoirs Action Plan* (FWCP 2020a). However, given that the study will collect data on Bull Trout, it will also contribute information to address priority # 13 (PEA.RLR.S04.RI.13) of the *Peace Region Rivers, Lakes, and Reservoirs Action Plan* (FWCP 2020a), particularly by filling in high immediacy data gaps 5.1a and 5.1b outlined in Table 5.1c in Hagen and Weber (2019).

3. Study Area

The project was conducted in the Parsnip River core area (watershed), with a focus on five streams: Parsnip River, Anzac River, Table River, Hominka River, and Missinka River. The Parsnip River watershed lies within the territory of the McLeod Lake Indian Band, Saulteau and West Moberly First Nations.

3.1. Parsnip River

The Parsnip River (54.769403°, −122.501018°) has a watershed area of 5,612 km^2 (Hagen et al. 2015). Total river length is 175 km, and the majority of this is low gradient. The river has a wide channel with many meanders, large gravel bars and clay banks. Substrate is a mix of cobble, gravel and fines. The Parsnip River and its major tributaries drain a mountainous area in the Hart Ranges of the Rocky Mountains, which lies east of the Rocky Mountain Trench. The Parsnip has turbid water as a result, and high peak flows from late-May to early June. Substantial glacial influence occurs in the Upper Parsnip River. However, in late summer downstream of the Missinka River (54.578597°, -122.034947°), turbidity improves (Hagen et al. 2015). The highest flows occur in late May, and the lowest flows occur during the period from September to March (Blackman 2002a). Discharge and temperature data are available from a hydrometric data gauge located above the confluence with the Misinchinka River (Station 07EE007, Water Survey of Canada).

3.2. Anzac River

The Anzac River (54.902632°, −122.280257°) drains a 939 km^2 watershed and is 78 km in length with an average gradient of 0.7% (Blackman 2002a). The stream drains a mountainous region of the Hart Ranges in the Rocky Mountains, on the East side of the Parsnip mainstem. Watershed elevation ranges from 730 m at the confluence with the Parsnip River to 2,495 m in the headwaters (Beaudry et al. 2000). The upper river is characterized by bedrock canyons with a moderate gradient (1-2%). The lower river lies in a wide unconfined valley. As the river nears the Parsnip River confluence it creates large meanders, many oxbows and has a low gradient (<0.5%) (Blackman 2002a). Snowmelt causes high river turbidity and flows in the spring months. However,

the Anzac River is low and clear in the late summer months and fall. Substrate is mainly composed of clean cobble and gravel. No hydrometric data are available for the Anzac River.

3.3. Table River

The Table River (54.755545°, −122.090737°) drains a 506 km^2 watershed and is 56 km in length with an average gradient of 0.7% (Blackman 2002a). The stream drains a mountainous region of the Hart Ranges in the Rocky Mountains, on the East side of the Parsnip mainstem. Watershed elevation ranges from 725 m at the confluence with the Parsnip River to 2500 m in the headwaters (Beaudry et al. 2000). The upper river has a moderate gradient (1-2%). The lower river has a low gradient (<0.5%) and contains many oxbows, side channels and abandoned channels (Blackman 2002a). No hydrometric data are available for the Table River.

3.4. Hominka River

The Hominka River (54.696944°, −121.837500°) drains a 433 km^2 watershed (Hagen et al. 2015). The stream drains a mountainous region of the Hart Ranges in the Rocky Mountains, on the East side of the Parsnip mainstem. Watershed elevation ranges from 669 m at the confluence with the Parsnip River to 2,100 m in the headwaters. The upper watershed is confined by steep slopes which quickly ascend to alpine terrain, and the river has a moderate gradient (3-5%). The lower river is sinuous, low gradient (<0.5%) and drains many adjoining marsh wetlands (Beaudry et al. 2000). No hydrometric data are available for the Hominka River.

3.5. Missinka River

The Missinka River (54.596666°, −121.737500°) drains a 434 km^2 watershed (Hagen et al. 2015). The stream drains a mountainous region of the Hart Ranges in the Rocky Mountains, on the east side of the Parsnip mainstem. Watershed elevation ranges from 740 m at the confluence with the Parsnip River to 2,346 m in the headwaters. The upper river is entrenched, confined by steep valley walls, and the river has a moderate gradient (1-3%). The lower river is sinuous, low gradient (<0.5%) with a wide alluvial floodplain (Beaudry et al. 2000). No hydrometric data are available for the Missinka River.

4. Methods

The methods used to address the study objectives include: acoustic telemetry, capture-recapture, temperature data logging, stable isotope analysis and spatial stream network modeling (SSNM). Arctic Grayling and Bull Trout were captured by angling. Captured fish were tagged (acoustic transmitters, and/or PIT [Passive Integrated Transponder] and anchor tags), sampled for muscle and adipose fin tissue (used in stable isotope analyses), and released. Fish tagged with acoustic transmitters were continuously monitored by an array of acoustic receivers deployed

throughout the Parsnip River watershed and in the Pack River. A small subset of potential prey for Arctic Grayling and Bull Trout were caught by angling, kick-netting and electrofishing, and sacrificed for stable isotope analysis (to fully characterize the food webs where Arctic Grayling and Bull Trout are located; see section 4.4). Data loggers were deployed throughout the Parsnip watershed to monitor both air and water temperature.

4.1. Fish Capture and Tagging

Arctic Grayling and Bull Trout were captured by angling (fly fishing or spin casting based on the current hatch and water conditions) at various sites in the Anzac, Table, Hominka, Missinka and Parsnip rivers beginning after freshet and ongoing until ice-up each year (Figure 1). Captured Arctic Grayling and Bull Trout > 230 g were surgically tagged with acoustic transmitters. For surgical tag implantation, the fish were sedated by electro-anaesthesia (Ward et al. 2017, Abrams et al. 2018) using electric gloves attached to a Transcutaneous Nerve Stimulation (TENS) 3000 unit (Koalaty Products Inc., Tampa, USA) or Smith-Root Electric Fish Handling Gloves (Smith-Root, Vancouver, USA), while kept in a V-shaped trough filled with ambient water. A small incision (20-30 mm) was made on the ventral midline 30-50 mm posterior to the pectoral fins and an acoustic tag (V9, Innovasea [formerly Vemco], Bedford, Canada) and a PIT tag (12mm HDX, Oregon RFID) were inserted into the peritoneal cavity. The incision was closed with 3-4 simple interrupted sutures (Wagner et al. 2011). The tags as well as the tagging instruments were all disinfected in a bath of Virkon (Lanxess, Germany) for 10 minutes and rinsed with distilled water. The fish were also externally tagged with an anchor tag (below the dorsal fin), measured (fork length), weighed and sampled for muscle and adipose fin tissue. After processing, the fish were placed into a recovery bag kept in the river so that ambient water continually flowed through it. Fish were released at the capture site after regaining equilibrium and responding vigorously when grabbed by the tail.

A total of 22 fish (16 Arctic Grayling and six Bull Trout) were tagged in 2021, (two Bull Trout in the Hominka River, three Arctic Grayling and one Bull Trout in the Missinka River, four Arctic Grayling and one Bull Trout in the Table River, nine Arctic Grayling and two Bull Trout in the Anzac River). All fish were tagged with acoustic transmitters, PIT tags and anchor tags. In total, 147 Arctic Grayling and 57 Bull Trout were tagged with acoustic transmitters across the watershed between 2018-2021.

To augment movement data on Arctic Grayling and Bull Trout, additional fish were captured and tagged with anchor and/or PIT (8mm FDX or 12mm HDX) tags, including fish < 230 g. The captured fish were immobilized by electro-anaesthesia (see above) and quickly handled in a V-shaped trough filled with ambient water, where it was externally tagged with an anchor tag (below the dorsal fin) and PIT tag (injected into the abdominal cavity), measured (fork length), weighed, and sampled for muscle tissue and adipose fin tissue. The location of capture or recapture of tagged fish was recorded with a GPS. A total of 38 additional fish (26 Arctic Grayling and 12 Bull Trout) were marked with anchor tags between 2018 and 2021. Three of these fish (two Bull Trout in the Parsnip River and one Arctic Grayling in the Anzac River) had pit tags added during capture. In an effort to increase the number of recaptures, local First Nations and recreational anglers were

asked to report the capture of any tagged fish as well as the date/time and spatial coordinates of capture. We also worked with the Angler's Atlas to use their MyCatch app and their capacity to reach out to thousands of anglers in BC to request that any tagged fish caught by anglers be reported along with the relevant information (date/time, location, and tag number).

Three fish were recaptured in 2021. Project staff recaptured one Arctic Grayling during the month of August in the Hominka River. An angler recaptured one grayling from the Table River during the month of July and another angler recaptured one grayling from the Table River in September. A total of 16 angler reports identifying recaptured fish (10 Arctic Grayling and six Bull Trout) tagged in the study were received between 2018 and 2021. Angler reports recaptured nine fish (six Arctic Grayling and three Bull Trout) in the Anzac River, six (four Arctic Grayling and two Bull Trout) in the Table River and one (Bull Trout) in the Williston Reservoir. Recaptured individuals were recorded and re-released pursuant to regional angling regulations which prohibit the recreational harvest of Arctic Grayling and Bull Trout from Williston tributaries.

Fish handling and tagging protocols were approved by the UNBC Animal Care and Use Committee (Protocol number: 2018-06). Permits to capture and tagging fish in this study were issued by the BC Ministry of Forests, Lands, Natural Resource Operations and Rural Development (Fish Collection Permit numbers: PG18-356580, PG19-523435, and PG20-606121).

4.2. Temperature Modeling

4.2.1. Field Data Collection

Air and water temperature data loggers (DS1921Z, Maxim Integrated, San Jose, USA; MX2201 and MX2203, Onset, Bourne, USA) were deployed throughout the study area from 2018-2021 (Figure 2). Water temperature loggers were attached to acoustic receiver moorings or boulders in the stream following methods outlined by Isaak et al. (2013). Air temperature loggers were installed 2 m off the ground on stable vegetation 0 m and 10 m from the stream. Inferences made from predicted temperatures can be greatly affected by the spatial proximity of sampled sites (Som et al. 2014). Therefore, optimal network design for the estimation of semivariance is critical for obtaining accurate and insightful conclusions from spatial data (Dale and Fortin 2014, Cressie et al. 2006). To accurately describe semivariance, a measure of spatial autocorrelation, it is required to include areas of high leverage in spatial trends (Zimmerman 2006). To meet this requirement in a dendritic river network, such as the Parsnip watershed, we spread temperature loggers over an elevational gradient and clustered loggers around confluences.

Over the study period there were 171 air (59) and water (112) temperature loggers site locations. In 2021, 14 water temperature data loggers were deployed in the watershed. Nine of these water temperature loggers were deployed with associated air temperature loggers. New deployments were placed where loggers were lost during spring freshet and at new locations to augment the network array used in the SSNM. In the fall of 2021, data from 62 water temperature loggers and 45 air temperature loggers were downloaded.

4.2.2. Data Cleaning and Imputation

Data collection and cleaning were conducted according to methods outlined by Sowder and Steel (2012). Some temperature records were incomplete for a variety of reasons including battery failure, exposure to air (water temperature loggers) and logger malfunctions. Time series with greater than 30% record completion during a temporal window of interest were imputed using a regularized iterative Principal Component Analysis algorithm implemented in the *missMDA* package in R Statistical Software (Josse and Husson 2016, R Core Development Team 2020). This data imputation technique creates a complete time series of daily mean air and water temperatures for each location. The algorithm implemented in the *missMDA* package minimizes and provides the mean square error of prediction (MSEP) for imputation using leave-one-out cross validation. The data loggers recorded a variety of sub-daily measurements, so data was aggregated into daily values before imputation. This technique of data imputation has a demonstrated history for temperature records and SSNM (Isaak et al. 2018).

4.2.3. SSNM Data Pre-processing

Spatial statistical models such as the SSNM require valid autocovariance functions to account for spatial autocorrelation among measurement locations. Due to the branching structure of river networks and the influence of downstream flow and tributary confluences, autocovariance functions need to be based on network distance, as patterns in spatial autocorrelation are not adequately described by Euclidean distance (Isaak et al. 2014). Specialized toolsets are required to fit spatial models to stream networks, which calculate a variety of watershed attributes including stream network distance, flow direction and landscape contributing areas. Before watershed attributes can be gathered, water temperature data was prepared in a points shapefile holding information on temperature metrics and data logging site locations.

A gridded air temperature raster layer at 1 km resolution was created with Universal Kriging in SAGA GIS (Conrad et al. 2015). Both air and water temperature data were aggregated across the time window of July 1st to September 15th. This time window represents the "feeding" window of adult Arctic Grayling seasonal migrations, which is a critical period for their growth (Northcote 1993). The feeding window was chosen based on historical movement studies (Blackman 2002b), and preliminary analysis of acoustic telemetry data using the actel package in R Statistical Software (Flavio and Baktoft 2020, R Core Development Team 2020). Data summaries which adequately describe relevant ecological contexts, termed as ecological facets, are critical in exploring relationships between temperature data and the ecology of species (Steel et al. 2017; Dahlke et al. 2020). The mean, maximum and standard deviation of the average weekly temperature values over the feeding window were calculated to produce three whole-season temperature metrics: 1) average weekly average temperature (AWAT), which describes mean conditions; 2) maximum weekly average temperature (MWAT), which describes extreme conditions; and 3) average weekly coefficient of variation (AWCV), which is a measure of variability around a mean temperature. Imputed daily average water temperatures were directly used in daily temperature prediction models.

The openSTARS package in R Statistical Software was used to produce a pre-processed stream layer (SSN object) (Kattwinkel and Szöcs 2018, R Core Development Team 2020). The openSTARS package uses R and GrassGIS (Neteler et al. 2012) to derive watershed attributes from a digital elevation model (DEM). Watershed attributes include stream network distance between temperature observation sites and flow direction. Additional landscape covariates created by the openSTARS package include upstream contributing area (H2OAreaA), elevation and slope. Watershed attributes, landscape covariates, observation data and spatial points for temperature prediction are combined and stored in the SSN Object which is used in a SSNM to generate temperature predictions.

4.2.4 Spatial Stream Network Model (SSNM)

Theory behind SSNM has greatly expanded over the past decade (Ver Hoef and Peterson 2010; Peterson and Ver Hoef 2010; Isaak et al. 2017). These models consider the spatial arrangement of watersheds (branching structure, directed flow, abrupt changes near tributary confluences) in ways that classical statistical approaches are unable to do (Isaak et al. 2010). Spatial statistical models such as the SSNM require valid autocovariance functions to account for spatial autocorrelation among measurement locations (Ver Hoef and Peterson 2010; Peterson and Ver Hoef 2010). Without accommodating for spatial autocorrelation, an inherent aspect of dendritic networks, traditional nonspatial models violate the assumption of independent random errors (Ver Hoef et al. 2006, 2014; Steel et al. 2016). Autocovariance functions need to be based on network distance (Isaak et al. 2014). To accommodate this Ver Hoef and Peterson (2010) developed tail-up (TU; flow-connected) and tail-down (TD; flow-connected and flow-unconnected) autocovariance models which are based on a continuous spatial analogue to moving averages for time series. These autocovariance functions allow for accurate description of spatial patterns based on hydrologic instead of simple Euclidean distance (Cressie et al. 2005; Peterson et al. 2013). By accommodating for flow directionality, branching structures, and weighting tributaries by size, SSNMs can accommodate multiple descriptions of spatial autocorrelation and borrow strength from relationships between monitored sites to minimize imprecision associated with temperature predictions using universal kriging on large river networks (Ver Hoef and Peterson 2010; Peterson and Ver Hoef 2010; Isaak et al. 2017). Multi-scale processes and interactions occur across river networks. Therefore, it is not uncommon to see multiple hydrologic and Euclidean patterns of spatial autocorrelation (e.g. among landscape attributes). To enhance predictive power, SSNMs can combine these autocovariance functions to produce mixed models based on covariates, variance components and random error through an extension of the basic spatial linear model:

$$\boldsymbol{y} = \mathbf{X}\boldsymbol{\beta} + \mathbf{z}_{TU} + \mathbf{z}_{TD} + \mathbf{z}_{E} + \boldsymbol{\varepsilon} \qquad \text{(eq. 1)}$$

where $\boldsymbol{y}$ is a vector of response variables, $\mathbf{X}$ is a matrix of covariates, $\boldsymbol{\beta}$ is a parameter vector, $\mathbf{z}_{TU}$ and $\mathbf{z}_{TD}$ are vectors of zero-mean random variables with a correlation structure based on the tail-up and tail-down stream network models, $\mathbf{z}_{\mathrm{E}}$ is a vector of zero-mean random variables with a correlation structure based on Euclidean distance and $\boldsymbol{\varepsilon}$ is a vector of independent random errors.

Model variable selection was based on a multi-stage process following methods outlined in Peterson and Ver Hoef (2010) and Marsha et al. (2021). Six predictor variables were evaluated for inclusion in the final models. Three variables including reach contributing area, mean elevation and mean slope represent watershed physical attributes. Three remaining variables included the air temperature metrics Air AWAT, Air MWAT, and Air AWCV. In stage one, predictor variables were selected using a threshold of inclusion. Evidence of no relationship ($p > 0.15$ for a two-sided *t*-test under a null hypothesis of zero slope) with the response metric (AWAT, MWAT or AWCV) resulted in removal of the predictor variable. In stage two, variables with variance inflation factor >2 were excluded from the model (Helsel and Hirsch 1992; Isaak et al. 2010; Marsha et al. 2021). The third stage was the selection of covariance parameters used to describe spatial autocorrelation among network connected, un-connected and Euclidean distances. A matrix was created with all possible combinations of covariance parameters in the SSN package. The combination of covariance parameters which yielded the lowest root mean squared prediction error was selected (Marsha et al. 2021). Following creation of the SSN object using openSTARS, the SSN package in R Statistical Software was used to fit and evaluate spatial statistical models (Ver Hoef et al. 2014, R Core Development Team 2020). The SSN package provides multiple diagnostic tools that were used for evaluating model fit. Residual plots were created to visualize residuals at observation sites or residual histogram plots. Leave-one-out cross validation statistics (root mean squared prediction error) were used to evaluate model performance. A generalized R-squared statistic was calculated for the fixed effects (Ver Hoef et al. 2014). Daily SSNM temperature predictions were used in the Spatial Capture Recapture Model (see section 4.3.3).

4.3 Monitoring of Fish with Acoustic Telemetry

4.3.1 Field Data Collection

Acoustic receivers (VR2W or VR2Tx, Innovasea [formerly Vemco], Bedford, Canada) were deployed widely across the watershed in clusters of 2-4 receivers spaced 0.5-2 km from one another (Royle et al. 2014). Receivers were moored hydrophone-up on the streambed using a system of concrete blocks, steel cable, and duckbill earth anchors. Given the narrow width of the streams (10-60m) in the study area and the typically high detection efficiency of acoustic receivers at short distances (< 50m), only one receiver was deployed at each point location at 5-20m from the banks. Data download windows were typically constrained to late summer and early fall by high water in the spring and early summer and difficult site access. As such, data collected by acoustic receivers from 2018-2019 were downloaded in 2019, data collected in 2019-2020 were downloaded in 2020, and data collected in 2020-2021 were downloaded in 2021.

4.3.2 Receiver Array Maintenance

The original acoustic array used in this study was installed in 2018 and consisted of 55 acoustic receivers deployed in the Parsnip River watershed and one receiver deployed in the Pack River watershed. The array grew in 2019, with an additional 26 acoustic receivers (including two replacements) deployed in the Parsnip River watershed and an additional two receivers in the lower Pack River (Figure 3).

Between 2018 and 2019, eight acoustic receivers were lost: seven to shifting sediment burying the receiver or exposing the anchor (four in the Table River; two in the Anzac River; one in the Parsnip River*)* and one was lost due to vandalism in the Parsnip River. The vandalized receiver was sent to Innovasea (formerly Vemco) for data download and repair and was not replaced, while two of the seven sites where receivers were lost to natural disturbance were deemed feasible for replacement (one in the lower Table River; one in the upper Anzac River). Deployment methods were adjusted after the 2018-2019 losses, with focus shifting from pool habitats (which were associated with sediment deposition and small, mobile sediments) to slow, deep run/glide habitats (which were associated with better receiver retention and larger, more stable cobble substrates).

Between 2019 and 2020, 21 additional acoustic receivers were lost due to an unusually high and sustained spring freshet which impacted the riverine environment to the point that some sites were no longer recognizable from the year before (seven in the Table River; five in the Parsnip River; four in the Anzac River; three in the Hominka River; two in the Missinka River; one in the Misinchinka River). After accounting for replaced and unreplaced losses, Arctic Grayling and Bull Trout tagged pursuant to this study were monitored by an array of 61 receivers.

Between 2020 and 2021, 10 acoustic receivers were lost. To replace array losses, 10 additional receivers were deployed from early July to early August (five in the Anzac River, three in the Table River, one in the Missinka River, and one in the Hominka River), all of which were successfully retrieved by the end of the study period in late September.

4.3.3 Spatial Capture Recapture Modeling

Telemetry data from 2019-2021 were analyzed using spatial capture-recapture models (SCR), a relatively recent extension of classical capture-recapture modeling in which the spatial explicitness of capture or detection locations is preserved (Royle et al. 2014; Borchers and Efford 2008). SCR is a class of hierarchical modeling in which a point process model of unobserved animal home range (or activity) centers is related to capture/detection data via an observation model of distance-dependent (imperfect) capture/detection process of individuals by the acoustic receiver array (Royle et al. 2018).

The point process model depicts an inhomogeneous Poisson point process estimating the unobserved activity centers of individuals moving about the environment. The probability density of an individual's home range center *X* can be estimated as (Efford 2008; Borchers and Efford 2008)

$$\hat{f}(X_i \mid \omega_i) = \frac{\widehat{Pr}(\omega_i|X_i)\hat{\pi}(X_i)}{\int_A \widehat{Pr}(\omega_i|X)\hat{\pi}(X)dX} \qquad \text{(eq. 2)}$$

where ω_i is capture/detection history of individual i; X_i is a random variable representing the Cartesian home range center for individual i; A is the summation of all points in the state-space (the area over which the probability density function is integrated); and $\hat{\pi}$ is the probability density of home range centers across the state-space.

The observation model (represented by the half-normal function) depicts the imperfect detection process of acoustic telemetry signals by the acoustic receiver array (Royle et al. 2014; Efford 2021). This SCR model formulation uses the river distance between state-space points rather than Euclidean distance, because the species targeted in this study are exclusively bound to the river network. The observation model is defined as (Efford 2008; Efford 2022)

$$g(d_{ij}) = g_0 e^{-\frac{d_{ij}^2}{2\sigma^2}} \qquad \text{(eq. 3)}$$

where d_{ij} is the network distance (meters) between the home range center of individual i and an acoustic receiver j; $g(d_{ij})$ is the probability of detection as a function of network distance between the home range center of individual i and a receiver j; g_0 is the intercept of the detection function; e is the Euler's (or natural) number (equal to 2.71828); and σ^2 is the scale parameter, which is a measure of spread on the distribution which can be interpreted as 95% of the activity area surrounding a home range center (Efford 2022).

To fit SCR models to a dataset, it is necessary to define the state-space — the area of potential habitat across the study region. Pixels of non-habitat, or in the case of fish, non-traversable habitat (i.e., land), are omitted from the state-space using a linear habitat mask (Efford 2022). The state-space for the Parsnip River watershed was defined as the Parsnip River and four of its major tributaries – the Anzac, Table, Hominka, and Missinka rivers. The Pack and Misinchinka rivers were omitted from the state-space because of their distance from the Parsnip core region (Pack) and low saturation of acoustic receivers (Misinchinka), which would affect parameter estimation. Each river in the state-space is defined from its mouth (into the Williston Reservoir for the Parsnip River and into the Parsnip mainstem for all other rivers) to its maximum extent of acoustic receiver coverage. An upstream buffer was added beyond each distal acoustic receiver to allow the model to accommodate individuals which leave detection range in the upstream direction before returning downstream. The habitat mask was defined as a shapefile in QGIS software (v3.16), imported into R using the rgdal package (Bivand et al. 2021), and discretized into 1 km segments. The result was a linear state-space defined by 366 spatially indexed pixels of potential habitat.

In addition to the state-space mask, there are two primary data structures associated with SCR models – the trap deployment file (TDF) and the encounter data file (EDF; Royle et al. 2014). The TDF is an R object of daily binaries (1/0) which indicate whether an acoustic receiver was active on any given day of the study (Efford 2021). Receivers that were inactive, lost, or removed within a given duration are accommodated by the SCR model by removing them from consideration during each evaluation of the observation model. The EDF is a data structure in which each tagged individual's encounter (detection) history is indexed by occasion and location (Royle et al. 2014). Together, the EDF and TDF are combined into a complex R object of 3D detection histories (Efford 2021). To construct the TDF and EDF in this study, detection data were queried from the database, filtered and restructured, reprojected into the state-space CRS (UTM Zone 10, CRS 32610), and organized into biweekly (over the feeding window) and monthly (for interannual population movement metrics) temporal bins for analyses.

A series of SCR models were fitted to the data to investigate the spatial distribution of Arctic Grayling home range center across different seasons. Metrics of ecological relevance (e.g. area use

around home range centers and degree of overlap) were derived from the model outputs and analyzed as observations in a time series to investigate longer-term pattern and process of the spatial ecology of Parsnip River Arctic Grayling. Spatial capture-recapture analyses for this study were conducted in R Statistical Software (R Core Development Team 2020) and made use of the packages secr, secrlinear, sf, tidyr, rgdal, igraph, lubridate, lookup, tidyverse, scales, gridExtra, and ggplot2 (Efford 2022, Efford 2021, Wickham et al. 2019, Bivand et al. 2021, Csardi and Nepusz 2006, Grolemund and Wickham 2011, Wright 2021, Wickham et al. 2019, Wickham and Seidel 2020, Auguie 2017, and Wickham 2016).

4.3.4. Integration of Spatial Covariates into the SCR Model, Model Fitting and Selection

4.3.4.1. Bull Trout densities

As a preliminary step before the SCR analyses of Arctic Grayling detection data, a series of SCR models were fit to individual Bull Trout encounter histories. Individual Bull Trout probability densities were estimated using the SCR null model (with no covariates). Probability densities were summed at each pixel in the state-space and divided by the number of individuals detected in the sampling window. The result was a relative probability density surface representing the sampled Bull Trout population (i.e., all individuals that were successfully detected by the telemetry array over the sampled window). These outputs were then included in the Arctic Grayling SCR state-space as a constant spatial covariate across the feeding window.

4.3.4.2. Thermal habitat

Fully integrated Arctic Grayling SCR models for which both temperature predictions from the SSNM and Bull Trout spatial data have been defined as covariates on the state-space were estimated approximately every two weeks during the trophic feeding window (July 1 – 15; July 16 – 31; Aug. 1 – 15; Aug. 16 – 31; Sep. 1 – 15). Temperature predictions were matched to each individual activity center and population means were compared to the mean value of pixel temperatures across the state-space. The scale parameter σ was extracted from each model for exploration of population-level movement trends over time.

*4.3.4.*3. Model Fitting

SCR models were fit using maximum likelihood methods to the Arctic Grayling data in 48 separate temporal windows: 12 single-month windows for 2019 and 2020 and nine in 2021 (the study ended in September 2021); and an additional 15 bi-weekly windows during the trophic period from July 1 – September 15 of each year (see break down in section 4.3.4.2). Of the 48 time windows, six had insufficient data (March and June 2019, November 2020, and January, February, and March of 2021). Of the remaining 42 windows, eight had enough data for the SCR model to estimate the locations of home range centers but were not to calculate the variance around the estimate (February, July, late July (trophic), and November of 2019, April, late August (trophic), and December of 2020, and July of 2021). The SCR model was also fitted to Bull Trout data (see section 4.3.4.1) within the same 48 temporal windows. However, the model failed to estimate to

estimate the variance in 11 time windows using the default algorithm. For these models, maximum likelihood estimation was skipped and the hessian and variance-covariance of the parameters were estimated as recommended in Efford (2022). Models that could not be fitted and models that could be fitted but failed to estimate the variance were discarded from further analyses.

There are three parameters estimated by SCR models: density of tagged fish in a river section (D), the scale parameter (σ), and the intercept of the detection function (g_0; Efford 2022). Parameters σ and g_0 are jointly used to estimate the detection function (observation model) defined above. The formula for the derived density parameter D is given as (Borchers and Efford 2008, Efford 2022)

$$\widehat{D} = \sum\left(a_i\hat{\theta}\right)^{-1} \qquad \text{(eq. 4)}$$

where $\hat{\theta}$ is the estimated effective sampling area for individual i with the detection parameter vector θ; and a_i is the individual-specific sampling area, calculated as $\int p.(X; z_i, \theta_i)dX$, where $p.(X)$ is the probability of the individual being detected at least once and z_i represents the covariates (Borchers and Efford 2008).

4.3.4.4. Model Selection with AIC

Candidate models estimating the relationships between D and different combination of temperature (Temp), Bull Trout densities (BT) and year (Year) were fitted to the data and the most parsimonious model was selected using the Akaike Information Criterion (Burnham and Anderson 2002).

*4.3.*5. Overlap Analyses

River habitat in this study is discretized as a linear feature (Efford 2021). The SCR state-space makes no accommodation for dealing with river width. More technically, the linear state-space is represented as a series of spatially-indexed point data. A convenient property of the pixels/points being indexed in this way is that probability density functions which integrate across the state-space can be plotted by pixel index and discretized by tributary when working in dendritic networks. For density functions which deal in comparable data on the same scale (e.g. SCR models of two co-occurring salmonid species), finding the degree of potential spatial overlap between the two becomes a simple task of finding the area shared beneath both probability curves *(sensu* Ridout and Linkie 2009).

Overlap analyses for this study were conducted by estimating the probability density functions of both Arctic Grayling and Bull Trout using the SCR methods described above and plotting them against their pixel index numbers. Spatial overlap at the watershed scale was estimated by finding the area of overlap under probability density curves for occurrence of Arctic Grayling and Bull Trout. The areas under the curve between each pixel pair were also calculated as an estimate of spatial overlap in each river.

For each overlap analysis, summary statistics comparing the mean fork lengths of each species were calculated and saved for analysis as a time series. As Bull Trout are gape-limited predators at 50% of their body size (Beauchamp and Van Tassell 2001) size ratios that exceed 2:1 Bull Trout to grayling at a given spatial location are more likely to be candidate sites for predation events to occur. Further, analyzing size of detected Bull Trout over time may indicate whether movement patterns might be attributed to fluvial or adfluvial Bull Trout subpopulations.

*4.3.*6. Exploration of Time Series

Summary statistics and the outputs of SCR models represent a snapshot of the tagged population state over a given temporal window. As both Arctic Grayling and Bull Trout in this study exhibit complex seasonal migrations, examining how estimated metrics change over time can reveal further insights into the migrations and potential trophic interactions of Arctic Grayling in the Parsnip River watershed. Metrics that were included for time series analysis include the scale parameter σ as an indicator of migration timing and movement magnitude; and the Bull Trout to Arctic Grayling mean size ratio as an indicator of the potential for trophic interactions to occur. Mean detected fish size was also examined to assess the intrusion of adfluvial Bull Trout into the system. Results from overlap analyses (see 4.3.5) at both the watershed- and tributary-scales were plotted as time series to visualize time windows in which the degree of overlap between the populations is elevated.

*4.3.*7. Individual Detection Histories

Spatial detection histories were grouped by year and by spatial frequency of detection to investigate the underlying behavior of individuals (of which the behavior of the population models is an emergent property). Individual detection histories were also used to easily assess which individuals showed evidence of migratory fidelity, mortality or tag loss, or potential use of the Williston Reservoir. Summary statistics of individual fish data were examined and reported as a percentage of the total number of tags deployed in each species.

4.4. Stable Isotope Analysis

4.4.1 Stable Isotope Sample Collection

Sampling for stable isotope analysis (SIA) occurred across the upper and lower reaches of the Anzac, Hominka, Table rivers, as well as the lower Missinka river. White muscle tissue and adipose fin samples were collected from Arctic Grayling and Bull Trout during acoustic transmitter implantation. Additionally, in 2020 several sites were angled for a total of 2 person-hours (2 anglers x 1hr effort) to target large, mature fish as well as systematically sampled for aquatic macro-invertebrates, other fish, periphyton and terrestrial vegetation (Figure 1). Benthic macro-invertebrates were sampled by conducting three rounds of 30 second kicknets in shallow riffles. Collected macro-invertebrates were then identified and stored for lab processing by genera. Potential prey fish such as Slimy Sculpin (*Cottus cognatus*), juvenile Burbot (*Lota lota*) and Mountain Whitefish (*Prosopium williamsoni*) were captured during kick netting or via

electrofishing, using a backpack electrofisher (LR-24, Smith-Root, Vancouver, WA, USA). Sampling was conducted along stream margins, beginning with conservative settings (100v, 40Hz, 10% duty cycle), then adjusted for optimal capture. Particulate organic matter was collected by scrubbing five large rocks in 3L of stream water for 30 seconds. Terrestrial vegetation was sampled by collecting the five most abundant riparian species. A large variety of samples is important to reduce uncertainty in dietary sources as well as provide insight into food web structure as small sample sizes can skew results of metrics (Layman et al. 2007).

4.4.2 Stable Isotope Sample Preparation and Analysis

In the laboratory, all collected material was kept in a –30°C freezer until processing for stable isotope analysis. Periphyton samples were filtered using a vacuum filtration system fitted with a fibreglass filter. All samples were dried in a standard laboratory convection oven set at 50°C for a minimum of 48 hours and then ground to a powder using a mortar and pestle. Measurements of $\delta^{13}C$ and $\delta^{15}N$ isotope from ground samples was done with a Delta Plus Continuous Flow Stable Isotope Ratio Mass Spectrometer (Thermo Finnigan, Bremen, Germany) coupled to a Carlo Erba elemental analyzer (CHNS-O EA1108, Carlo Erba, Milan, Italy) at the Environmental Isotope Laboratory, University of Waterloo (Waterloo, ON).

4.4.3 Stable Isotope Data Analysis

SIA is a common method used to investigate ecosystem food webs, determine trophic interactions between species and diet analysis, all done by looking at $\delta^{13}C$ and $\delta^{15}N$ ratios (e.g. Harrison et al. 2017, Estrada et al. 2003). R Statistical Software packages such as *SIBER* (Stable Isotope Bayesian Ellipses in R) have been developed to estimate dietary breadth and dietary overlap from stable isotope data (Jackson et al. 2011, Layman et al. 2007). *SIBER* is considered a powerful tool and accurate method of understanding trophic relations and niches, as isotope enrichment in tissues increases with trophic level (Jackson et al. 2011, France 1995). SIA using ellipses creates an accurate analysis of consumer diet with resulting ellipse variance representing among individual variation in diet (Harrison et al. 2017, Semmens et al. 2009). Ellipses are chosen as they can be used to determine niche similarity among species or communities (Jackson et al. 2011, Layman et al. 2007).

Basic isoplots fitted with 95% confidence ellipses were plotted and a set of comparative metrics such as total ellipse area and standard ellipse area corrected for small sample sizes (Layman et al. 2007) were calculated for both Arctic Grayling and Bull Trout, as well as with invertebrates and prey fish. Total ellipse area (TA) and standard ellipse area corrected for a small sample size (SEA_c), were calculated to provide insight on trophic positioning between species and at a larger scale (Jackson et al. 2011, Layman et al. 2007). An unequal variances *t*-test was conducted in order to determine differences in levels of carbon and nitrogen between Bull Trout and Arctic Grayling. Residuals were assessed for normality using Q-Q plots. Homogeneity of variance was assessed using Levene's test. Ultimately, all data tested met the assumptions of the *t*-test. A general linear model was fitted to the fork length, C isotope and N isotope data to determine patterns of dietary preferences among size classes in a species. These varied analyses enabled us to investigate

differences not only between species but also among varying size classes within species. All analyses were done using R Statistical Software (R Core Development Team 2020).

5. Results and Outcomes

5.1. Temperature Modeling

5.1.1. Temperature Data Imputation and Summary Metrics

Data were available from 39 logger locations in 2018 for late summer (August 1-September 15) revealing a mean temperature of 11.9ºC (± 2.9ºC). After data imputation, a total of 55 complete water temperature times series in 2019, 48 in 2020 and 37 in 2021 were used to compute water temperature metrics and included in the SSNM. The MSEP for water temperature data imputation was 0.17ºC for 2019, 0.19ºC for 2020 and 0.75ºC for the 2021 data. The mean of the three thermal metrics at water observation sites in 2019 were 10.53ºC (± 1.37ºC) for AWAT, 11.70ºC (± 1.61ºC) for MWAT and 0.06 (± 0.01) for AWCV. The mean of the three thermal metrics at water observation sites in 2020 were 9.26ºC (± 1.84ºC) for AWAT, 12.50ºC (± 2.45ºC) for MWAT and 0.08 (± 0.01) for AWCV. The mean of the three thermal metrics at water observation sites in 2021 were 11.39ºC (± 2.70ºC) for AWAT, 14.24ºC (±3.63ºC) for MWAT and 0.06 (± 0.01) for AWCV.

Data collection and imputation yielded a total of 21 complete air temperature times series in 2019, 17 in 2020 and 20 in 2021. These air temperature time series were used to compute air temperature metrics and construct the air temperature raster layer used in the SSNM. The MSEP for air temperature data imputation was 0.65ºC for 2019, 0.82ºC for 2020 and 1.14ºC for the 2021 data. The mean of air temperature metrics in 2019 were 11.9ºC (± 1.2ºC) for AWAT, 13.5ºC (± 1.3ºC) for MWAT and 0.14 (± 0.05) for AWCV. Mean air temperature metrics in 2020 were 11.1ºC (± 1.3ºC) for AWAT, 16.1ºC (± 1.1ºC) for MWAT and 0.18 (± 0.06) for AWCV. Mean air temperature metrics in 2021 were 13.2ºC (± 1.1ºC) for AWAT, 21.8ºC (± 1.8ºC) for MWAT and 0.15 (± 0.05) for AWCV. Leave one out cross validation computed a small prediction error for Universal Kriging of the raster layer relative to air temperature fluctuation (Table 1).

5.1.2. Spatial Stream Network Model

In most models, only air temperature and reach contributing area were retained as predictor variables, in other cases air temperature was the sole retained predictor variable (Table 2). In the 2019 feeding window five of six predictor variables were retained by the model selection procedure. Reach contributing area was not related to the response metric AWCV ($p > 0.15$), so it was removed for that model. For the 2020 data air temperature metrics and reach contributing areas passed the first stage of model selection. The air temperature metrics AWAT, MWAT and elevation were not related to the response metric AWCV, so were removed for that model. In the 2021 feeding window, air AWAT and AWCV were retained. Following stage two of the variable

selection process, examination of the variance inflation factor, slope and elevation were removed because they exceeded the threshold VIF >2.

No single mix of predictor variables and covariance parameters could most accurately predict the three different response metrics in each year. Spatial Stream Network Models were fit for the 2019-2021 feeding windows (July 1st – September 15th) AWAT, MWAT, AWCV and daily average temperature response metrics. Each model had a low root mean squared prediction error (RMSPE) and standardized bias (Table 2). The presented R^2 value only represents the variance composition attributable to the predictor variables and not the spatial covariance parameters, which comprise the remaining variance composition. Daily SSNM models performed well using the air AWAT predictor variable. RMSPE varied daily but remained at values near those reported for whole-season metrics and exceedances were minor relative to values reported in Table 2 (Appendix B). Predicted and observed temperatures had a close spread around the equivalence line (Figure 4; Appendix B). Histograms of leave-one-out cross validation residuals and spatial residual plots showed patterns at certain sites where fitted models were over or underpredicting (Figures 5 and 6). For the 2021 data, the models overpredicted in high elevation cold tributaries.

Two prominent patterns are apparent in the thermal landscape of the Parsnip River. The first is that elevation gradients dominate the thermal landscape at the watershed scale. High elevation, low stream order drainages on the eastern side of the watershed are a critical cold-water supply to the entirety of the river drainage. The low elevation streams on the western side of the watershed supply a warmer input and in warm climatic conditions produce thermal habitat near or exceeding values suitable for Arctic Grayling (i.e., > 14.5 °C). This pattern is particularly notable in the AWAT and MWAT metrics in 2020 and 2021 (Figure 7). The second most prominent pattern is that the within-year coefficient of variation was consistently higher in small, high elevation streams. Unexpectedly, whole-season AWCV differed significantly among years. The years 2019 and 2021 showed similar patterns in AWCV in which different tributaries had more (Anzac, Table Rivers) or less (Hominka River) variation around the mean temperature. Importantly this pattern was not ubiquitous across the entire watershed and substantial variation in AWCV was seen across years and among tributaries. Daily SSNM predictions depict the high amount of thermal habitat variability across the summer trophic feeding window (see link for animation in Appendix B). An expected pattern across the three years of the study shows gradual warming with a peak in warm temperatures in late July and early August and a gradual cooling towards September. What these animations reveal is the high amount of variability summarized by the AWCV metrics. This variability is caused by multiple instantaneous shifts in thermal habitat which vary in magnitude and timing across all three years of the study.

5.2. Acoustic Telemetry Monitoring

5.2.1. Summary of Detections and Temperature Use by Arctic Grayling

In the 2019, 2020 and 2021 feeding windows there were, respectively, 390,748 (across 62 receiver sites), 140,977 (47 receiver sites), and 121,997 (45 receiver sites) detections of acoustic tagged fish. Average daily temperature at sites with Arctic Grayling occurrence was 10.8ºC (± 1.3ºC), 9.4ºC (± 1.9ºC), and 11.2ºC (± 2.3ºC) in 2019, 2020 and 2021, respectively.

The distribution of temperatures at sites with Arctic Grayling detections was narrower than the distribution of temperatures across all receiver sites (Figures 8 to 10). Moreover, the median temperature at sites with Arctic Grayling detections was lower than the median temperature across all receiver sites (Figures 8 to 10). This suggests that Arctic Grayling occur at a narrower and slightly colder range of temperatures than what is available in the Parsnip River thermal landscape. Importantly the median temperatures and ranges shift interannually due to variable climatic conditions.

5.2.2. Description of Arctic Grayling Movements

Of the 129 Arctic Grayling whose data were available to be included in the SCR analyses, 18 (14%) were filtered out for low detections, suspected mortality, depredation, or possible expulsion of the acoustic tag after surgery. Of the remaining individuals (n = 111) which had a detection history spanning multiple years (n= 84), a majority of detection histories displayed high tributary fidelity (n = 54; 64.3%), migrating from the Parsnip mainstem into the same tributary for two or three consecutive years. Some individuals (n = 21; 25%) showed use of multiple tributaries across years, with a subset of these (n = 10; 11.9%) showing much greater range than their conspecifics, ranging well into two or more tributaries and traversing a larger range within the Parsnip mainstem. Of the individuals which showed multiple tributary use, a subset of individuals (n = 9; 10.7%) showed use of both the lower Anzac and Missinka Rivers, while others used multiple tributaries with no discernible pattern. No Arctic Grayling tagged in this study were observed migrating into the nearby Pack River, and only three individuals (2.7%) were observed downstream of the Misinchinka River near the Parsnip mouth at the Williston Reservoir (between late summer and early winter).

For the 15 bi-weekly feeding window models in which temperature predictions were done, the SCR model where density of tagged grayling was related to an additive effect of the distribution of thermal habitat and Bull Trout (model D ~ Temp + BT) was selected as the best model by AIC (Table 4). For remaining longer-term (monthly) windows, the SCR model where density of tagged Arctic Grayling was related to density of tagged Bull Trout only (model D ~ BT) was selected (Table 4).

Over the course of any given year, Arctic Grayling in the Parsnip River watershed overwinter in the Parsnip River mainstem, with some intrusions into the lower reaches of the tributaries, in particular the Anzac River (Figure 11). Beginning in April and May, individual movements become more frequent, though distribution is still limited to the middle and lower reaches of the tributaries and retention in the Parsnip mainstem is still common (Figure 12). By July, Arctic Grayling distributions begin to include the uppermost reaches in the state-space, indicating their maximal summer range has been realized (Figure 13). In August, Arctic Grayling movements start to become decentralized, with home range centers identified along the Parsnip mainstem and all reaches of the tributaries (Figure 14). This distribution pattern lasted well into September for all years in the study. By October, Arctic Grayling home range centers begin to gather in the Parsnip mainstem once again, with most individuals returning to their winter ranges by November (Figure

15). Figures here are chosen as good representations of these distributions. A full set of figures with SCR model outputs can be found in Appendix A.

5.2.3. Overlap Analyses

Analysis of the Bull Trout detection data showed an increase in mean fork length of tagged fish in the Parsnip River watershed beginning in April and May of all years. Mean fork lengths ranged from <400 to 550 mm during the winter months and from 500 – 700 mm during the summer months (Figure 16). As Arctic Grayling population fork lengths stay relatively the same through time, this increase corresponds with an increase in the Bull Trout to Arctic Grayling size ratio in the summer months. The summer months also see an increase in spatial overlap at both the watershed and tributary scales (Figures 17 to 19). Overlap plots as well as a guide for interpreting them can be found in Appendix A.

To assess how changing Bull Trout distribution (based on tagged fish only) may influence overlap analyses, individual Bull Trout detection histories were assessed and grouped into apparent Williston reservoir users and populations that appear to be resident to the Parsnip River watershed (Figure 20). Resident Bull Trout had a mean fork length of 441.2 mm (± 84.7, n = 10), while Williston Reservoir Bull Trout had a mean fork length of 633.0 mm (± 138.8, n = 14). However, there was a second apparent resident population that emerged, and these were counted separately because they were about 37% larger than the other residents (606.0 ± 113.1 mm, n = 9; $t = 3.5$, $P = 0.002$,), but not as large as the adfluvial population. This subset of Bull Trout seems to exclusively use the Hominka River and overwinter in the Parsnip mainstem near the Hominka confluence. Four individuals were observed using the nearby Pack River (735.25 ± 157.7 mm). Interestingly, mean size of detected Bull Trout also increased year-over-year, though the mechanism behind this observation is uncertain and may be related to tagging of larger Bull Trout in later years of the study.

5.3. Stable Isotope Analysis

A total of 466 biological samples were collected for isotopic analysis of carbon ($\delta^{13}C$) and nitrogen ($\delta^{15}N$) between 2018-2021 (Table 3). Samples included adipose fin tissue (n = 210), muscle tissue (n = 99), prey fish (n = 41), invertebrates (n = 30), terrestrial vegetation (n = 70) and aquatic vegetation or periphyton (n = 16).

When comparing Bull Trout and Arctic Grayling dietary breath using the total ellipse area (TA) from fitted stable isotope biplots (Figure 21), Bull Trout were found to occupy a larger dietary niche in comparison to Arctic Grayling ($TA_{\text{Bull Trout}} = 24.1$, $TA_{\text{Arctic Grayling}} = 10.5$). This pattern was also revealed by standard ellipse area corrected for small sample size (SEA_c) ($SEA_{c\ \text{Bull Trout}} = 8.7$, $SEA_{c\ \text{Arctic Grayling}} = 2.4$). These data indicate that Bull Trout consume a diverse selection of dietary items while Arctic Grayling exhibit more homogeneous dietary preferences among individuals (Figure 21). A stable isotope biplot was also used to investigate food web positioning of Arctic Grayling and Bull Trout (Figure 22). Bull Trout were found to occupy the top trophic position with Arctic Grayling being the next highest. The trophic position of potential prey fish registered slightly below that of Arctic Grayling.

Significant differences in mean isotopic carbon (t = 4.20, df = 48, P < 0.001) and nitrogen (t = -10.64, df = 47, P < 0.001) between Arctic Grayling and Bull Trout were identified (Figures 23 and 24). Mean $\delta^{15}N$ levels were measured at 7.32‰ for Arctic Grayling and 10.74‰ for Bull Trout (Figure 23). Mean $\delta^{13}C$ levels in Arctic Grayling were calculated at –28.12‰ and Bull Trout were measured at –30.01‰ (Figure 24). A linear regression revealed no relationship between Arctic Grayling $\delta^{15}N$ and fork length (F = 0.77, df = 92, P = 0.38) (Figure 25), but a positive relationship between $\delta^{15}N$ and fork length in Bull Trout (β = 0.093, 95% CI [0.079, 0.11], t = 7.57, P < 0.001, R^2 = 0.51, Figure 26).

5.4. Community Outreach

The project team coordinated six outreach activities in 2021-2022:

i. Presentation of the spatial stream network model and thermal habitat use by Arctic Grayling at the Canadian Conference for Fisheries Research in the Fish Movement Symposium by Bryce O'Connor February 25, 2022.
ii. Discussion of preliminary results and progress update to Ministry of FLNRORD fisheries branch staff by Dr. Eduardo Martins, Joseph Bottoms, Ian Clevenger and Bryce O'Connor March 31, 2021.
iii. Presentation of estimating detection efficiency of acoustic receivers deployed in the Parsnip River watershed using machine learning at UNBC Research Week by Devon Smith March 2, 2022.
iv. Over the study period 10 tagged grayling and 6 Bull Trout were recaptured by recreational anglers and reported to the research team. These interactions involved explanation of the project, acknowledgement of FWCP funding and education and outreach about the Parsnip River Watershed.
v. Communication with McLeod Lake Indian Band (Maggie McDonald) is ongoing and coordinated with other FWCP funded projects implemented by Chu Cho Environmental LLP.
vi. Presentation of project through collaboration with the UNBC Offices of Research & Innovation and Recruitment to EBUS Academy students. December 9, 2021

6. Discussion

6.1. Temperature Modeling and Spatio-Temporal Patterns in Thermal Habitat

Spatial Stream Network Models predicted continuous water temperatures and allowed insights into aquatic thermal habitat availability across the entire Parsnip River watershed. SSNM's were used to predict a continuous aquatic thermal landscape in 1 km stream length intervals for daily average temperatures and three whole-season temperature metrics. These metrics were summarized during the Arctic Grayling trophic feeding window (July 1st - Sep 15th), which is a critical period for individual growth (Northcote 1993). Thermal landscape maps revealed that thermal habitat availability within the Parsnip River Watershed was favourable for adult Arctic Grayling in 2019 and 2020. However, thermal habitat availability was more constrained in 2021

and in specific instances in 2020 (Figure 7, Appendix B). The results corroborate findings in other large watersheds with strong elevation gradients (e.g. Isaak et al. 2016; Steel et al. 2017). High elevation, small order streams act as critical cold-water supply and climate refugia in extreme conditions. These streams, despite their predicted vulnerability to warm air temperatures, are acting as climate refugia for native cold-water temperate ectotherms (Isaak et al. 2016). SSNMs for the Parsnip River watershed show variation in thermal habitat availability which needs to be considered if management methods based on thermal thresholds are implemented (Steel et al. 2017).

6.1.1 Field Data Collection

Temperature loggers deployed in 2021 bolstered the existing sampling design in the Anzac, Table, Parsnip, Hominka, Missinka, Misinchinka, Reynolds, Colbourne, Wichcika, Bills, Firth and other smaller (unnamed) watersheds. Including smaller streams and new deployments along elevation gradients increased the predictive power of the SSNM. Temperature monitoring array expansion and maintenance was a necessary step to create accurate autocovariance functions required to build the SSNMs (Som et al. 2014). The drawbacks of this spatial model's large minimum sample size are greatly outweighed by the benefits of the temperature maps and associated predictions which can supply the information needed to support regionally significant resource conservation decisions (Isaak et al. 2014). By communicating with other organizations implementing projects funded by the FWCP, this team has been able to leverage access to deployment sites on critical habitats for Bull Trout which have a large impact on downstream thermal habitat gradients. By expanding the monitoring arrays spatial reach, we have been able to gain insight into the model's predictive ability as the monitoring array's spatial configuration has evolved over the study period. The model leans heavily on the spatial pattern among monitored sites to create accurate predictions. Areas of high leverage and disjunctions in the moving average pattern between flow-connected sites (tributary confluences) have a large impact on prediction accuracy.

6.1.2 Temperature Data Imputation and Model Evaluation

Data imputation using a regularized iterative principal component analysis algorithm continues to be an effective method to complete time series of temperature data when technological failure occurs due to logger issues or natural events. Data inadequacies often inhibit complete dataset analysis and the low MSEP of the imputation is a positive indication of its utility (Isaak et al. 2018).

The variety of covariance parameters used in final SSNMs is testament to the thermal variability across years and metrics. This has been noted in other studies modeling thermal ecological facets (Marsha et al. 2021). The RMSPE was low (<1) across all 125 combinations of covariance parameters tested in stage three of model selection. This consistently low prediction error reinforces the ability of the models to predict accurate thermal landscapes. The spatial covariance parameters are a key strength to SSNMs and evidence of their superior prediction accuracy over

non-spatial models has been well documented (Peterson et al. 2013; Isaak et al. 2014). Leave one out cross-validation (LOOCV) residuals were chosen as a diagnostic statistic instead of a raw residual which does not include the effect of the covariance parameters. LOOCV Residuals had a normal distribution centered around zero, which had variable spatial patterns across the monitoring array (Figures 5 and 6). The spatial residual plots for AWCV showed very little pattern.

Temperature variability is heavily influenced by stream-reach scale (localized) hydrologic complexity (Webb et al. 2008). Watershed scale hydrologic processes like the predictor variables used in these models may not be the best estimators of variability metrics. This outcome is interesting and requires more research into what hydrological features that influence site variability can be gathered in a GIS using remote sensing techniques. This is important in watersheds like the Parsnip River where large-scale field programs are logistically difficult to implement. For AWAT and MWAT there was little pattern in spatial predictive accuracy across years.

As temperature magnitude and variability increased from 2019-2021, the size of the monitoring array decreased, and predictive accuracy also declined. These observations outline the importance of network array design and attaining the recommended minimum sample size of 50-100 loggers in large watersheds (Isaak et al. 2014). Caution should be used when interpreting results of spatial statistical models predicting areas far from monitoring arrays. Prediction accuracy in the tributaries and mainstem which hold Arctic Grayling critical habitats was high given that they were a focus of the array. Despite this, the models performed very well due to our suitable sample sizes (Table 2). Model diagnostics suggest that abundant spatial information was available within the monitoring array to support accurate predictions.

6.1.3 Spatial Stream Network Model

Graphical depictions of thermal habitat availability highlight the complexity of the watershed in ways traditional data summaries are unable to do. Not only is there heterogeneity across the watershed in a single instance of time (Appendix B), but also across years and temperature metrics (Figure 7). Empirical data summaries or averaged summaries of thermal regime lack the spatial scope to display the complexity of thermal habitat that aquatic ectotherms have access to (Steel et al. 2017). The reported averages for MWAT 2019 (11.70ºC), 2020 (12.50ºC) and 2021 (14.24ºC) indicate a warming trend over the study period, however predictions from the SSNMs depict very different thermal seasons (Figure 7, Appendix B). In 2019 small temperature increases in the mainstem Parsnip and lower tributaries were periodic through the summer, whereas in 2020 temperatures stayed lower with one week of heightened temperatures in late July and early August. During the warmest year of the study in 2021, periodic temperature increases were similar to those in 2019, but were higher in magnitude. The spatial patterns of variability in the watershed are also presented eloquently by the SSNMs as opposed to traditional data summaries. The difference in AWCV across three seasons depicts a stark contrast (Figure 7). Variability relative to the mean was highest in 2020 which only had one week of heightened temperatures. Variability in 2019 and 2021 was more expected with high coefficient of variation in tributary streams relative to the mainstem Parsnip. This variability is caused by multiple instantaneous shifts in thermal habitat

which vary in magnitude and timing. Importantly though coefficient of variation predictions still showed different spatial patterns between the tributaries in 2019 and 2021.

Predicted water temperatures exceeded literature derived critical upper thermal limits for Arctic Grayling (18ºC) in 2020 and 2021 (LaPerriere and Carlson 1973; Coutant 1977; Lohr et al. 1996). In 2019 the maximum stream reach prediction (17.24ºC, Parsnip River) approached the 18ºC upper avoidance limit cited by Contant (1977). Predictions warmer than reported Arctic Grayling thermal occurrence range in the Williston watershed (2.5-14.5ºC; Ballard and Shrimpton 2009; Hawkshaw et al. 2014) occurred mostly in the low elevation streams, particularly small tributaries on the western side of the Parsnip mainstem. These tributaries are not known to hold large populations of Arctic Grayling but are suggested to ephemerally provide habitat for younger life stages (Stamford et al. 2017). Thermal exceedances in the Parsnip mainstem extended upstream from the Reservoir to the confluence with the Missinka River. During instantaneous warm water periods the lower tributaries on the east side of the mainstem rose above reported thermal occurrence ranges (14.5ºC). However, for most of the summer east side tributaries draining high elevation streams remained important cold-water inputs to the low elevation mainstem river (Figure 7, Appendix B). In the feeding window of 2019 and 2020, cold-edge limits were more likely an impediment to Arctic Grayling distribution than warm-edge limits which appear limiting in 2021.

Elevational gradients supply cold-water to critical summer habitats in the tributaries on the east side of the Parsnip mainstem (Figure 7). In mid-summer, a clear isotherm shift occurs during warm, dry conditions where these critical, lower elevation summer habitats see chronic increases in temperature (Appendix B). Although short-lived, these events may lead to elevated thermal stress for cold-water adapted species. Such variability in thermal conditions, in addition to mean temperatures, should be considered in management decisions. It is well documented that high variation at temperatures near upper thermal preferences can have negative effects on species which will differentially impact various life stages and life history tactics (Morash et al. 2021). Monitoring water temperature and calculation of variability in addition to average metrics should continue in order to advise landscape management decisions which impact aquatic thermal habitat. Landscape management decisions in areas of inconstant thermal habitats should consider the downstream implications of possible disturbances such as forest canopy removal, which has a demonstrated history of increasing stream temperatures (Caissie 2006). The importance of high elevation, low stream order reaches which supply cold water to the critical feeding habitats for adult Arctic Grayling will be paramount in more extreme climatic conditions and need to be prioritized for conservation. This will be critical to ensure species like Arctic Grayling and Bull Trout have a buffer against the rapid and more variable air temperature increases forecasted over the remainder of the century (Isaak et al. 2015).

6.2. Telemetry Data Modeling and Arctic Grayling Spatial Ecology

Spatial capture-recapture models provided a prediction of individual and population home range centers in the Parsnip River watershed, and metrics derived from a series of SCR models provided information about the influence of thermal habitat availability as well as spatial and temporal overlap with Bull Trout on Arctic Grayling movement and distribution. While these are

powerful statistical tools, some care must be taken when interpreting the ecological relevance of their outputs. For example, the state-space of the SCR models makes no accommodation for ice conditions during the winter months. Despite this, it performed reasonably well at limiting Arctic Grayling movements to the presumably ice-free regions of the state-space throughout the study. This is evidenced by the model predicting middle-tributary home range centers in the springtime while the population movement metrics would suggest a push further upstream. This can be attributed to the dependence on the model of individual detection histories.

The spatial ecology of the sampled Arctic Grayling population in the Parsnip River watershed is complex and has three distinct phases: overwintering, spring spawning, and summer feeding. Overwintering assemblages of Arctic Grayling in the Parsnip River mainstem are concentrated in the reaches near the confluences of the four study tributaries and includes some use of the lower Parsnip River between the Anzac confluence and Colbourne Creek (an insight that was not well observed during preliminary non-SCR analyses reported in previous years). Springtime movements are sudden and wide-ranging, with individuals beginning to push into the middle tributaries around ice-out and freshet in April and May. This is consistent with the spawning migration described in Hagen and Stamford (2017). Increased movements along the Parsnip mainstem during this time suggest a switch from winter residency to migratory behavior regardless of if the individual has entered its spawning tributary yet.

The decentralization of home range centers during the summer months from mainly tributary use to watershed-level use is consistent with a switch to the feeding window in which Arctic Grayling disperse in search of feeding territories. Detecting the switch between searching and feeding behaviors is difficult as Arctic Grayling are apparently known to migrate in search of more favorable feeding habitat if access to their current habitat is reduced or impeded by sediment (Stamford et al. 2017). However, July of all years showed a reduction in the scale parameter (95% of the home range area) compared to its neighboring months, which could indicate a reduction in range as individuals settle down to form hierarchical feeding groups (Hughes 1992, Hughes and Reynolds 1994). Analyses of the SSNM-integrated population models over the feeding window showed that Arctic Grayling preferred areas slightly cooler (10.0 ± 1.3 °C) than the mean temperatures across the state-space (10.9 ± 1.5 °C). Summer distribution patterns persist until October, at which time Arctic Grayling begin congregating in the Parsnip River mainstem once more, reaching an approximately winter distribution by November.

The breakdown of Arctic Grayling into single-tributary and multi-tributary users revealed some interesting population traits. While most individuals display high tributary fidelity, one-quarter of the total population appeared to display what could be likened to a straying phenotype in Pacific salmon (Keefer and Caudill 2014). These individuals remain in the Parsnip River watershed, though between years they do not return to the same reaches that their location of tagging and prior detection history would suggest. Of these, a distinct subset emerged (n = 10; 11.9% of the sample population) which showed ranges much broader than their conspecifics, spending time in two or more of the study tributaries and ranging further downstream in the Parsnip mainstem than others. It is unknown whether this is an adaptive migratory strategy to habitat stressors or a population-level mechanism for genetic dispersal.

Three individual Arctic Grayling were detected in the Parsnip River within 5 Rkm of the Williston Reservoir, although it is unclear from their detection histories whether they entered the reservoir before returning upstream towards the Parsnip River watershed. It is also worth noting that these three individuals were counted as part of the far-ranging multi-tributary population discussed above. While the SCR models cannot directly answer the question of whether Arctic Grayling use the Parsnip reach of Williston Lake (Stamford et al. 2017), because there were no acoustic receivers deployed in Williston Lake, track histories may provide clues about the lower Parsnip River or potential reservoir use of these individuals. The first Arctic Grayling, a 379 mm male (tag GR19305) was detected near the reservoir for four days between January 1 – 5, 2020 before moving back towards the Parsnip core area. The second, a 310 mm female (GR19358), was detected near the reservoir on October 22, 2020, and not again until April 24 of the following spring. The third, a 356 mm female (GR24372), was detected near the reservoir on August 3, 2019, again on November 1, and then is not detected again until May 21 of the following year back towards the Parsnip core area. Detection histories of these and other individuals can be found in Appendix A.

Overlap analyses with Bull Trout provided a relatively coarse look at the spatiotemporal potential for trophic interactions between the two species. As the predictive range of the SCR model is related to the number of tags deployed (and detected) across the state-space, analysis windows with relatively few detections (e.g. July 16 – 31 2021) may falsely lead the reader to conclude that little overlap occurs during a given window, while it is more appropriate to interpret this as little overlap was *detected*. It is interesting to note that the referenced modeling window also aligns with the decreased scale parameter for Arctic Grayling in July, which furthers evidence that individuals may have settled into reaches where they're not frequently in proximity with the acoustic receivers.

Bull Trout detection data shows a pattern of larger, adfluvial fish entering the Parsnip River watershed from the Williston Reservoir beginning in April after which the overlap between species remains elevated until September. Analysis of overlap frequencies did not appear to generate a clear pattern of spatial niche, although there does seem to be some segregation of the populations temporally, with each population using given areas in the upper watershed at different times. This is more likely attributed high upper tributary use by Bull Trout during their fall spawning migration than any interspecific interactions.

Overlap analyses alone are not adequate to assess predation risk, so population size ratios were compared over time to aid interpretation. Because of the winter emigration of adfluvial Bull Trout from the state-space, winter predation risk is relatively low, when the size ratio between the populations was relatively minor. In the summer months, size ratios began to approach the 50% threshold for Bull Trout gape limitation (Beauchamp and Van Tassell 2001), though population means rarely crossed it. For these reasons, it seems likely that opportunistic predation events of Bull Trout on Arctic Grayling may occur during the summer months, though mean population fork lengths suggest that this will be limited to sub-adult and adult Arctic Grayling and Bull Trout on the lower and upper peripheries of their respective size distributions, and that sub-adult and adult Arctic Grayling are not a staple food source for Bull Trout in the Parsnip River watershed.

6.3. Trophic Relationships between Arctic Grayling and Bull Trout

6.3.1 Comparison of Bull Trout and Arctic Grayling Dietary Isotopes

It has been well established that $\delta^{15}N$ changes at a consistent rate between trophic positions (Adams and Sterner 2000, France 1995). Most studies account for a 3.4‰ change in $\delta^{15}N$ positions (France 1995), though there is debate as to how this value changes between species and communities (Adams and Sterner 2000). We found significant differences in $\delta^{15}N$ concentrations between Arctic Grayling and Bull Trout, indicating both species rely on different dietary inputs. Prey sources at the same trophic level as Arctic Grayling appear to contribute to Bull Trout diet as their $\delta^{13}C$ levels align. Additionally, mean $\delta^{15}N$ for Bull Trout is 3.4‰ more enriched than grayling (10.74‰ vs 7.32‰). Bull Trout and Arctic Grayling diets differ in source when considering terrestrial vs aquatic derived inputs. Not surprisingly, our findings of differences in $\delta^{13}C$ and $\delta^{15}N$ concentrations mean that adult Bull Trout and Arctic Grayling have distinct diets. Furthermore, small (juvenile and sub-adult) Arctic Grayling likely contribute to Bull Trout (particularly those large enough to not be gape limited to consume Arctic Grayling) diet in part with other potential prey fish. This is consistent with previous studies that have noted Bull Trout preying on Arctic Grayling and other similar prey fish, especially as Bull Trout grow larger in length (McPhail and Baxter 1996).

6.3.2 Dietary Analyses Based on Fork Length

Our results confirm that size and life history are likely main drivers in individual dietary patterns of both Arctic Grayling and Bull Trout as seen in other studies on the species (Moore and Kenagy 2004, McPhail and Baxter 1996). Juvenile or smaller Bull Trout are likely feeding on lower trophic levels being primarily insectivorous before switching to larger prey such as whitefish, sculpin and Arctic Grayling. This is thought to happen at around 110 mm in fork length (McPhail and Baxter 1996, Guy et al. 2011). Stream resident Bull Trout are also hypothesized to be primarily insectivorous (McPhail and Baxter 1996), while fluvial and adfluvial individuals consume high protein diets, composed primarily of fish that may be up to 50% of their body length (Beauchamp and Tassell 2001). These high energy requirements are likely due to the increased energetic costs of high movement and or the need to acclimate to variable stream temperatures. Differences in life history and body size explain the large dietary variation shown by Bull Trout in our study. Bull Trout that are isotopically similar to Arctic Grayling may be resident or smaller individuals, consuming benthic invertebrates as they cannot outcompete fluvial and adfluvial fish for larger prey items. Additionally, the Bull Trout at the higher end of the $\delta^{15}N$ spectrum may be preying upon resident or juvenile Bull Trout, Arctic Grayling, or whitefish, given their substantially higher $\delta^{15}N$ levels. Having a large sample or population primarily composed of fluvial Bull Trout would explain the large variation in individual diets as their foraging tendencies are regarded as primarily opportunistic, switching between prey fish and invertebrates depending on abundance and competition (McPhail and Baxter 1996). Adfluvial Bull Trout that feed in the reservoir likely

explain the two individuals that are outside of the calculated breadth as they appear to consume higher amounts of lacustrine derived nutrients (lower $\delta^{13}C$) than the sample mean.

Arctic Grayling are regarded as primarily insectivorous foragers with terrestrial invertebrates being important dietary items both seasonally and as fish grow larger (Zuev et al. 2017, Stewart et al. 2007a). Juvenile diets primarily consist of zooplankton and small invertebrates (Schmidt and O'Brien 1982, Stewart et al. 2007a). As individuals grow larger, they rely on seasonally available invertebrates found in summer feeding tributaries (Stewart et al. 2007a). Aquatic larvae and pupae are regarded as important year-round prey while other dietary items that belong to the Orders Diptera and Ephemeroptera are seasonally important (Zuev et al. 2017). Competition between Bull Trout and Arctic Grayling is thought to primarily occur when juvenile Bull Trout adopt an insectivorous diet similar to that of Arctic Grayling (Hagen and Stamford 2017, Northcote 1993). This is apparent in Figures 25 and 26 where we can see Bull Trout at the smaller end of the size range exhibiting similar $\delta^{15}N$ concentrations as adult Arctic Grayling. This is supported by Larkin (1956), who reasoned that species may have similar diets but feed at different sites. Bull Trout and grayling likely have reduced interspecific competition through use of different habitats and also may be separated by differing thermal preferences similar to what has been noted in this study population and other Bull Trout populations (Isaak et al. 2017; Heinle et al. 2021). Crock et al. (2003) found that when Arctic Grayling move into summer feeding areas, they exhibit site fidelity, staying within 300 m of their feeding territory. Bull Trout, however, are known to undergo extensive migrations from winter feeding areas to cold spawning habitat (McPhail and Baxter 1996). Temporal differences may also be influencing dietary competition, as Arctic Grayling and Bull Trout life histories are extremely diverse in the system, resulting in times of increased and decreased co-occupancy of streams. This further supports the idea that Bull Trout and Arctic Grayling exhibit patterns of sympatric resource partitioning, though there are almost certainly times of increased competition, such as periods of low resource availability (Lakse et al. 2018).

6.3.3 Foodweb Level Analysis

Potential prey fish and Arctic Grayling overlap in dietary items, which has been noted in the literature as both Arctic Grayling and potential prey fish, consume aquatic benthic organisms such as invertebrate larvae (Whiteley 2007). When comparing Arctic Grayling and potential prey fish, Arctic Grayling appear to incorporate more terrestrial derived nutrients as their diet on average appears to be less enriched with $\delta^{13}C$ (Hoeinghaus and Zeug 2008). Our results align with previous studies that highlight low level producers such as aquatic invertebrates as lowest in $\delta^{15}N$ while top predators such as Bull Trout exhibit the highest $\delta^{15}N$ levels (Alvarez and Ward 2019). It appears that competition for similar dietary resources is not the strongest driver of dietary interactions in the Parsnip River watershed. Although most taxa overlap in terms of dietary breadth, core species diets appear significantly different.

7. Recommendations

This study has revealed complexity in thermal habitat availability, distribution, movement and resource use of Arctic Grayling and Bull Trout in the Parsnip River watershed. We have gathered information relevant to key population attributes that can be used to prioritize conservation action planning for Arctic Grayling (data gaps 5.1.3a-I in Table 6 of Stamford et al. 2017). Outcomes of this study primarily addressed priority action # 9 (PEA.RLR.S03.RI.09) of the *Peace Region Rivers, Lakes, and Reservoirs Action Plan* (FWCP 2020a). The FWCP has a vision for thriving fish and wildlife populations in watersheds that are functioning and sustainable. To achieve this goal, conservation of natural patterns of thermal habitat variability and population life-history diversity in the Parsnip watershed must be prioritized.

Thermal habitat variability across the Parsnip River watershed was discovered across multiple temporal scales which influences the distribution of Arctic Grayling. While findings on the watershed scale provide foundation for understanding the spatial ecology of Arctic Grayling, sub-watershed scale thermal habitat will further inform how conservation actions could be designed to preserve cold-water thermal habitat for the species. Future thermal habitat investigations should continue to be coordinated with existing abundance and critical habitat monitoring projects (i.e., PEA-F22-F-3407, PEA-F22-F-3408, PEA-F22-F-3424).

High elevation, small streams supply cold-water to critical habitats for Arctic Grayling and Bull Trout. Tributary streams and adjacent land should be immediately prioritized for conservation actions. Water temperature increases are expected not only due to ongoing climate change but also given the high level of industrial resource activity in the Parsnip River watershed. Such activities can change the landscape in ways that result in increasing water temperatures and sedimentation, which are known to negatively impact Arctic Grayling (Stamford et al. 2017). Results from this report, Hagen et al. (2015), Hagen and Weber (2019), Stamford et al. (2017) and other FWCP funded projects (i.e., PEA-F22-F-3407, PEA-F22-F-3408, PEA-F22-F-3424) should be used to address priority actions PEA.CRE.S01.LS.03 *Prioritize areas for land securement* and PEA.CRE.S01.LS.04 *Conduct Land Securement* from the Peace Region Cross-Ecosystem Action Plan (FWCP 2020b).

Habitat conservation actions have benefits which cross the riparian divide of aquatic and terrestrial habitats and provide a buffer against extreme climatic conditions and human disturbance expected over the next century, which will negatively affect all FWCP priority species. The BC Ministry of Forests should additionally prioritize angling closures in Bull Trout critical spawning habitats which have become accessible due to recent industrial activity. Priority should be placed on the Anzac and Table Rivers which are undergoing rapid habitat degradation due to cumulative effects of stressors (climate change, logging, pipeline development) and increasing angling pressure. Our final recommendations are:

1. Prioritize conservation actions in and around small high elevation tributaries which provide cold-water inputs to downstream critical habitats for Arctic Grayling and provide spawning and rearing habitat for Bull Trout

2. Immediately prioritize areas for land securement and conservation actions which can preserve thermal habitat within the Parsnip River watershed and reduce the impacts of cumulative stressors

3. Pursue research on thermal habitat patterns at sub-watershed scales which may affect the ability of Arctic Grayling and Bull Trout to thermoregulate

4. Align thermal habitat monitoring programs across scales (sub-watershed to basin-wide) to ensure insights at multiple spatial and temporal scales in the Williston Reservoir watershed

5. Integrate critical habitat (including findings of this research) and abundance monitoring programs to investigate habitat covariates which affect the spatial distribution and temporal dynamics of priority species for FWCP

6. Investigate Arctic Grayling genetic diversity in the Parsnip River watershed and determine its influence on movement behaviours and thermal adaptative capacity

7. Coordinate partnerships across multiple organizations (First Nations, Provincial Government, public stakeholders and Academia) which share common goals to support research and implementation of conservation actions

8. Acknowledgements

A large number of people provided critical support to different phases of this project: Julian Napoleon, Daniel Scurfield, Rioghnach Steiner, Grayson Vanderbyl, Cale Babey, Daniel Larson, Luc Turcotte, Douglas Thompson, John Orlowsky, Kendra Robinson, Bruna Gonçalves, Daniel Erasmus, Brian Smith, Tom Wilms, Nikolaus Gantner, Ian Spendlow, Ray Pillipow, Zsolt Sary, John Hagen, Dawn Cowie, Michael Stamford, Duncan McColl, Jeff Strohm, Kari Van Ruskenveld, Matthew Blackburn, Ainsley Davison, Alex Bevington, Jean Bowen, Hunter Gleason, Liz Hirsch, Derek Gilbert, Sydney Schutz, Amanda Carrier, and Rebecca Lahti. The Ministry of Forests kindly provided us with helicopter access to remote sites of the study area. This project is funded by the Fish and Wildlife Compensation Program (FWCP). The FWCP is a partnership between BC Hydro, the Province of BC, Fisheries and Oceans Canada, First Nations and public stakeholders to conserve and enhance fish and wildlife in watersheds impacted by BC Hydro dams. This research took place in the territory of the McLeod Lake Indian Band, Saulteau and West Moberly First Nations.

9. References

Abrams, A. E. I., A. M. Rous, J. L. Brooks, M. J. Lawrence, J. D. Midwood, S. E. Doka, and S. J. Cooke. 2018. Comparing immobilization, recovery, and stress indicators associated with electric fish handling gloves and a portable electrosedation system. Transactions of the American Fisheries Society 147:390–399.

Alvarez, J.S., Ward, D.M. 2019. Predation on wild and hatchery salmon by non-native brown trout (*Salmo trutta*) in the Trinity River, California. Ecology of Freshwater Fish. DOI: 10.1111/eff.12476

Allen, A. M., and N. J. Singh. 2016. Linking movement ecology with wildlife management and conservation. Frontiers in Ecology and Evolution 3:1–13.

Auguie, B. 2017. gridExtra: Miscellaneous Functions for "Grid" Graphics. R package version 2.3. https://CRAN.R-project.org/package=gridExtra.

Ballard. S and J.M. Shrimpton. 2009. Summary Report of Arctic Grayling Management and Conservation 2009. A synopsis of the information available on Arctic Grayling in the Omineca region of northern British Columbia and identification of additional information needs. Peace/Williston Fish and Wildlife Compensation Program Report No. 337.

Beauchamp, D.A., Van Tassell, J.J. 2001. Modeling Seasonal Trophic Interactions of Adfluvial Bull Trout in Lake Billy Chinook, Oregon. Transactions of the American Fisheries Society. 130(2): 204-216.

Beaudry P. and Associates, EDI Environmental Dynamics Inc. 2000. Parsnip River Watershed Restoration Plan and Priority Assessment Project. Report prepared for: Canadian Forest Products Ltd., 5162 Northwood Pulp Mill Road, Prince George, BC.

Bivand, R., Keitt, T., and Rowlingson, B. 2021. Rgdal: Bindings for the 'Geospatial' data abstraction library. R package version 1.5-28.

Blackman, B. G. 2002a. The distribution and relative abundance of Arctic Grayling (Thymallus arcticus) in the Parsnip, Anzac and Table rivers. Peace/Williston Fish and Wildlife Compensation Program, Report No. 254. 15pp.

Blackman, B. G. 2002b. Radio Telemetry Studies of Arctic Grayling Migrations to Overwinter, Spawning and Summer Feeding Areas in the Parsnip River Watershed 1996-1997. Peace/Williston Fish and Wildlife Compensation Program, Report No. 263.

Borchers, D. L. and Efford, M. G. (2008) Spatially explicit maximum likelihood methods for capture–recapture studies. Biometrics, 64, 377–385.

Burnham K.P., and Anderson D.R. 2002. Model Selection and Multimodel Inference: A Practical Information-Theoretic Approach. 2nd edition. Springer, New York.

Clarke, A. D., K. H. Telmer, and M. Shrimpton. J. 2007. Elemental analysis of otoliths, fin rays and scales: A comparison of bony structures to provide population and life-history information for the Arctic Grayling (Thymallus arcticus). Ecology of Freshwater Fish 16:354– 361.

Conrad, O., Bechtel, B., Bock, M., Dietrich, H., Fischer, E., Gerlitz, L., Wehberg, J., Wichmann, V., and Bohner, J. (2015): System for Automated Geoscientific Analyses (SAGA) v. 2.1.4, Geosci. Model Dev., 8, 1991-2007, doi:10.5194/gmd-8-1991-2015.

Cooke, S. J., E. G. Martins, D. P. Struthers, L. F. G. Gutowsky, M. Power, S. E. Doka, J. M. Dettmers, D. A. Crook, M. C. Lucas, C. M. Holbrook, and C. C. Krueger. 2016. A moving target—incorporating knowledge of the spatial ecology of fish into the assessment and management of freshwater fish populations. Environmental Monitoring and Assessment 188:239.

Coutant, C. C. 1977. Compilation of temperature preference data. Journal of the Fisheries Research Board of Canada 34: 739-745.

Cressie, N., Frey, J., Harch, B., and Smith, M. 2006. Spatial prediction on a river network. J Agric Biological Environ Statistics 11(2): 127–150. doi:10.1198/108571106x110649.

Csardi G, Nepusz T: The igraph software package for complex network research InterJournal, Complex Systems 1695. 2006. https://igraph.org

Dahlke, F.T., Wohlrab, S., Butzin, M., and Pörtner, H.-O. 2020. Thermal bottlenecks in the life cycle define climate vulnerability of fish. Science 369(6499): 65–70. doi:10.1126/science.aaz3658.

Dale, M. R. T. & Fortin, M-J. 2014. Spatial Analysis: A Guide for Ecologists. Cambridge University Press, Cambridge, UK.

Efford, M. G. (2021). secrlinear: Spatially Explicit Capture--Recapture for Linear Habitats.R package version1.1.4. https://CRAN.R-project.org/package=secrlinear/.

Efford, M. G. (2022). secr: Spatially explicit capture-recapture models. R package version 4.5.0. https://CRAN.R-project.org/package=secr.

Evangelista, C., Bioche, A., Lecerf, A., Cucherousset, J. 2014. Ecological opportunities and intraspecific competition alter trophic niche specialization in an opportunistic stream predator. Journal of Animal Ecology. 83(5): 1025-1034.

Flávio, H., and Baktoft, H. 2020. actel: Standardised analysis of acoustic telemetry data from animals moving through receiver arrays. Methods in Ecology and Evolution. doi:10.1111/2041-210x.13503.

France, R.L. 1995. Differentiation between littoral and pelagic food webs in lakes using table carbon isotopes. Limnology and Oceanography. 40(7): 1310-1313.

FWCP. 2020a. Fish and Wildlife Compensation Program – Peace Regions. Rivers, Lakes, and Reservoirs Action Plan. BC Hydro, Prince George, BC.

FWCP. 2020b. Fish and Wildlife Compensation Program – Peace Regions. Cross-Ecosystem Action Plan. BC Hydro, Prince George, BC.

Grolemund, G., and Wickham H. 2011. Dates and Times Made Easy with lubridate. Journal of Statistical Software, 40(3), 1-25.

Guy, C.S., McMahon, T.E., Fredenberg, W.A., Smith, C.J., Garfield, D.W., Cox, B.S. 2011. Diet Overlap of Top-Level Predators in Recent Sympatry: Bull Trout and Nonnative Lake Trout. Journal of Fish and Wildlife Management. 2(2): 183-189.

Hagen, J., and M. Stamford. 2017. FWCP Arctic Grayling Monitoring Framework for the Williston Reservoir Watershed. Fish and Wildlife Compensation Program - Peace Region, Prince George.

Hagen, J., and S. Weber. 2019. Limiting Factors, Enhancement Potential, Critical Habitats, and Conservation Status for Bull Trout of the Williston Reservoir Watershed: Information Synthesis and Recommended Monitoring Framework. Fish and Wildlife Compensation Program - Peace Region, Prince George.

Hagen, J., S. Williamson, M. D. Stamford, and R. Pillipow. 2015. Critical Habitats for Bull Trout and Arctic Grayling within the Parsnip River and Pack River watersheds. Report prepared for: McLeod Lake Indian Band, Sekani Drive, McLeod Lake, BC.

Harrison, P.M., Gutowsky, L.F.G., Martins, E.G., Ward, T.D., Patterson, D.A., Cooke, S.J., M. Power. 2017. Individual isotopic specializations predict subsequent inter-individual variation in movement in a freshwater fish. Ecology. 98(3): 608-615.

Hastings, A., S. Petrovskii, and A. Morozov. 2011. Spatial ecology across scales. Biology Letters 7:163–165.

Hawkshaw, S. C. F., M. P. Gillingham, and J. M. Shrimpton. 2014. Habitat characteristics affecting occurrence of a fluvial species in a watershed altered by a large reservoir. Ecology of Freshwater Fish 23:383–394.

Heinle, K.B., Eby, L.A., Muhlfeld, C.C., Steed, A., Jones, L., D'Angelo, V., Whiteley, A.R., and Hebblewhite, M. 2021. Influence of water temperature and biotic interactions on the distribution of westslope cutthroat trout (*Oncorhynchus clarkii lewisi*) in a population stronghold under climate change. Canadian Journal of Fisheries and Aquatic Sciences 99(999): 1–13. doi:10.1139/cjfas-2020-0099.

Helsel, D.R., and Hirsch, R.M. 1992. Statistical Methods in Water Resources. Elsevier Science, New York.

Hoeinghaus, D.J., Zeug, S.C. 2008. Can stable isotope ratios provide for community-wide measures of trophic structure? Comment. Ecological Society of America. 89(8): 2353-2357.

Hughes, N.F. 1992. Ranking of Feeding Position by Drift-Feeding Arctic Grayling (*Thymallus arcticus*) in Dominance Hierarchies. Canadian Journal of Fisheries and Aquatic Sciences. 49: 1994-1998.

Hughes, N. F., & Reynolds, J. B. (1994). Why do Arctic Grayling (*Thymallus arcticus*) get bigger as you go upstream? Canadian Journal of Fisheries and Aquatic Sciences, 51(10), 2154–2163.

IPCC. 2014. Climate Change 2014: Synthesis Report. Contribution of Working Groups I, II and III to the Fifth Assessment Report of the Intergovernmental Panel on Climate Change. Edited by Core Writing Team, R.K. Pachauri, and L.A. Meyer. Intergovernmental Panel on Climate Change, Geneva, Switzerland.

Isaak, D. J., C. H. Luce, B. E. Rieman, D. E. Nagel, E. E. Peterson, D. L. Horan, S. Parkes, and G. L. Chandler. 2010. Effects of climate change and wildfire on stream temperatures and salmonid thermal habitat in a mountain river network. Ecological Applications 20:1350–1371.

Isaak, Daniel J., Horan, Dona L., and Wollrab, Sherry P. 2013. A simple protocol using underwater epoxy to install annual temperature monitoring sites in rivers and streams. General Technical Report RMRS-GTR-314. U.S. Department of Agriculture, Forest Service, Rocky Mountain Research Station, Fort Collins, CO.

Isaak, D.J., Peterson, E.E., Hoef, J.M.V., Wenger, S.J., Falke, J.A., Torgersen, C.E., Sowder, C., Steel, E.A., Fortin, M., Jordan, C.E., Ruesch, A.S., Som, N., and Monestiez, P. 2014. Applications of spatial statistical network models to stream data. Wiley Interdisciplinary Reviews: Water 1(3): 277–294.

Isaak, D.J., Young, M.K., Nagel, D.E., Horan, D.L., and Groce, M.C. 2015. The cold-water climate shield: delineating refugia for preserving salmonid fishes through the 21st century. Global Change Biology 21(7): 2540–2553.

Isaak, D.J., Young, M.K., Luce, C.H., Hostetler, S.W., Wenger, S.J., Peterson, E.E., Hoef, J.M.V., Groce, M.C., Horan, D.L., and Nagel, D.E. 2016. Slow climate velocities of mountain streams portend their role as refugia for cold-water biodiversity. Proceedings of the National Academy of Sciencies 113(16): 4374–4379. doi:10.1073/pnas.1522429113.

Isaak, D.J., Wenger, S.J., and Young, M.K. 2017. Big biology meets microclimatology: defining thermal niches of ectotherms at landscape scales for conservation planning. Ecological Applications 27(3): 977–990. doi:10.1002/eap.1501.

Isaak, D.J., Luce, C.H., Chandler, G.L., Horan, D.L., and Wollrab, S.P. 2018. Principal components of thermal regimes in mountain river networks. Hydrological and Earth System Sciences 22(12): 6225–6240. doi:10.5194/hess-22-6225-2018.

Jackson, A.L., R., Inger, Parnell, A.C., and S. Bearhop. 2011. Comparing isotopic niche widths among and within communities: SIBER - Stable Isotope Bayesian Ellipses in R. Journal of Animal Ecology. 80(1): 595-602.

Josse, J., and Husson, F. 2016. missMDA : A Package for Handling Missing Values in Multivariate Data Analysis. Journal of Statistical Software 70(1), 1-31.

Kattwinkel M, Szöcs E. 2018 openSTARS: open source implementation of the STARS ArcGIS toolbox. See https://github.com/MiKatt/openSTARS.

Keefer, M. L., & Caudill, C. C. (2014). Homing and straying by anadromous salmonids: A review of mechanisms and rates. *Reviews in Fish Biology and Fisheries*, *24*(1), 333–368. https://doi.org/10.1007/s11160-013-9334-6

Kurylyk, B. L., K. T. B. MacQuarrie, T. Linnansaari, R. A. Cunjak, and R. A. Curry. 2015. Preserving, augmenting, and creating cold-water thermal refugia in rivers: concepts derived from research on the Miramichi River, New Brunswick (Canada). Ecohydrology 8:1095–1108.

Larkin, P.A. 1956. Interspecific Competition and Population Control in Freshwater Fish. Journal of the Fisheries Research Board of Canada. 13(3):327-342.

Layman, C.A., D.A. Arrington, C.G. Montaña, and D.M. Post. 2007. Can stable isotope ratios provide for community wide measures of trophic structure? The Ecological Society of America. 88(1):42-48.

Lucas, M. C., and E. Baras. 2001. Migration of Freshwater Fishes. Blackwell Science Ltd, Oxford.

Magnan, P., Fitzgerald, G.J. 1984. Mechanisms responsible for the niche shift of brook charr, *Salvelinus fontinalis* Mitchill , when living sympatrically with creek chub, *Semotilus atromaculatus* Mitchill. Canadian Journal of Zoology. 62(8): 1548-1555.

Marsha, A.L., Steel, E.A., and Fullerton, A.H. 2021. Modeling thermal metrics of importance for native vs non-native fish across stream networks to provide insight for watershed-scale fisheries management. Freshwater Science: 000–000. doi:10.1086/713038.

McPhail, J.D., Baxter, J.S. 1996. A review of Bull Trout (*Salvelinus confluentus*) life history and habitat use in relation to compensation and improvement opportunities. British Columbia Ministry of Environment, Lands and Parks, Fisheries Management Report No. 104: 40p.

Milinsky, M. 1982. Optimal Foraging: The Influence of Intraspecific Competition on Diet Selection. Behavioral Ecology and Sociobiology. 11: 109-115.

Moore, J.W., Kenagy, G.J. 2004. Consumption of shrews *Sorex spp*. by Arctic Grayling, *Thymallus arcticus*. Canadian Field Naturalist. 118(1): 111-114.

Morash, A.J., Speers-Roesch, B., Andrew, S., and Currie, S. 2021. The physiological ups and downs of thermal variability in temperate freshwater ecosystems. Journal of Fish Biology. doi:10.1111/jfb.14655.

Neteler M, Bowman MH, Landa M, Metz M. 2012. GRASS GIS: a multi-purpose open source GIS. Environmental Modeling and Software. 31: 124 –130. doi:10.1016/j. envsoft.2011.11.014.

Northcote, T.G. 1993. A review of management and enhancement options for Arctic Grayling (Thymallus arcticus) with special reference to the Williston Reservoir in British Columbia. British Columbia Ministry of Environment, Lands and Parks, Fisheries Management Branch. Report no. 101:69p.

Ogburn, M. B., A.-L. Harrison, F. G. Whoriskey, S. J. Cooke, J. E. Mills Flemming, and L. G. Torres. 2017. Addressing challenges in the application of animal movement ecology to aquatic conservation and management. Frontiers in Marine Science 4:70.

Pearce T and Abadzadesahraei S (2019). First Nations Information Gathering on Kokanee, Bull Trout and Arctic Grayling: report for the Tsay Keh Dene Nation. Prince George, FWCP and ArcticNorth Consulting, 24pp.

Peterson, E.E., and Ver Hoef, J.M. 2010. A mixed-model moving-average approach to geostatistical modeling in stream networks. Ecology 91(3): 644–651. doi:10.1890/08-1668.1.

QGIS.org, 2022. QGIS Geographic Information System. QGIS Association. http://www.qgis.org

R Development Core Team. 2020. R: A Language and Environment for Statistical Computing, R Foundation for Statistical Computing: Vienna, Austria. ISBN 3-900051-07-0.

Ridout, M., and Linkie, M. 2009. Estimating overlap of daily activity patterns from camera trap data. Journal of Agriculture, Biological, and Environmental Statistics 14(3), 322-337.

Royle, J. A., Chandler, R. B., Sollmann, R., & Gardner, B. (Eds.). 2014. Spatial capture-recapture. Elsevier.

Royle, J. A., A. K. Fuller, and C. Sutherland. 2018 Unifying population and landscape ecology with spatial capture-recapture. Ecography 41:444–456.

Schmidt, D., O'Brien, J. 1982. Planktivorous Feeding Ecology of Arctic Grayling (*Thymallus arcticus*). Canadian Journal of Aquatic Sciences. 39(3): 475-482.

Semmens, B.X., Ward, E.J., Moore, J.W., Darimont, C.T. 2009. Quantifying Inter- and Intra-Population Niche Variability Using Hierarchical Bayesian Stable Isotope Mixing Models. PLoS ONE. 4(7): e6187

Som, N.A., Monestiez, P., Hoef, J.M.V., Zimmerman, D.L., and Peterson, E.E. 2014. Spatial sampling on streams: principles for inference on aquatic networks. Environmetrics 25(5): 306–323.

Sowder, C., and Steel, E.A. 2012. A Note on the Collection and Cleaning of Water Temperature Data. Water 4(3): 597–606.

Stamford, M., J. Hagen, and S. Williamson. 2017. Limiting Factors, Enhancement Potential, Conservation Status, and Critical Habitats for Arctic Grayling in the Williston Reservoir Watershed, and Information Gaps Limiting Potential Conservation and Enhancement Actions. Fish and Wildlife Compensation Program - Peace Region, Prince George.

Stamford, M. D., and E.B. Taylor. 2005. Population subdivision and genetic signatures of demographic changes in Arctic Grayling (Thymallus arcticus) from an impounded watershed. Canadian Journal of Fisheries and Aquatic Sciences 62: 2548–2559.

Steel, E.A., Beechie, T.J., Torgersen, C.E., and Fullerton, A.H. 2017. Envisioning, Quantifying, and Managing Thermal Regimes on River Networks. Bioscience 67(6): 506–522. doi:10.1093/biosci/bix047.

Stewart, D. B., N. J. Mochnacz, C. D. Sawatzky, T. J. Carmichael, and J. D. Reist. 2007a. Fish diets and food webs in the Northwest Territories: Bull Trout (Salvelinus confluentus). Canadian Manuscript Report of Fisheries and Aquatic Sciences. Pages vi–18p.

Stewart, D. B., N. J. Mochnacz, J. D. Reist, T. J. Carmichael, and C. D. Sawatzky. 2007b. Fish diets and food webs in the Northwest Territories: Arctic Grayling (Thymallus arcticus). Canadian Manuscript Report of Fisheries and Aquatic Sciences. Pages vi–21p.

Ver Hoef, J.M., Peterson, E.E., Clifford, D., and Shah, R. 2014. SSN : An R Package for Spatial Statistical Modeling on Stream Networks. Journal of Statistical Software 56(3).

Wagner, G. F., S. J. Cooke, R. S. Brown, and K. A. Deters. 2011. Surgical implantation techniques for electronic tags in fish. Reviews in Fish Biology and Fisheries 21:71–81.
Ward, T. D., J. W. Brownscombe, L. F. G. Gutowsky, R. Ballagh, N. Sakich, D. McLean, G. Quesnel, S. Gambhir, C. M. O'Connor, and S. J. Cooke. 2017. Electric fish handling gloves provide effective immobilization and do not impede reflex recovery of adult largemouth bass. North American Journal of Fisheries Management 37:652–659.
Whiteley, A.R. 2007. Trophic polymorphism in a riverine fish: morphological, dietary and genetic analysis of Mountain Whitefish. Biological Journal of the Linnean Society. 92(2): 253-267.
Wickham, H. 2016. ggplot2: Elegant Graphics for Data Analysis. Springer-Verlag New York
Wickham et al., (2019). Welcome to the tidyverse Journal of Open Source Software, 4(43), 1686 https://doi.org/10.21105/joss.01686
Wickham, H., and Seidel, D. 2020. scales: Scale Functions for Visualization. R package version 1.1.1.
Wright, K. (2021). lookup: Functions Similar to VLOOKUP in Excel. R package version 1.0.
Wrona, F.J., Davies, R.W., Linton, L., Wilkialis, J. 1981. Competition and coexistence between *Glossiphonia complanata* and *Helobdella stagnis* (*Glossiphoniidae: Hirudinoidea*). Oecologia. 48: 133-137
Zimmerman, D.L. 2006. Optimal network design for spatial prediction, covariance parameter estimation, and empirical prediction. Environmetrics 17(6): 635–652. doi:10.1002/env.769.
Zuev, I.V., Shulepina, S.P., Trofimova, E.A., Zotina, T.A. 2017. Seasonal Changes in Feeding and Relative Condition Factors of Arctic Grayling (Thymallus arcticus) in a Stretch of the Middle Reaches of the Yenisei River. Contemporary Problems of Ecology. 10(3): 250-258.

Table 1. Prediction error (ºC) produced by leave-one-out cross validation for air temperature raster layers created using Universal Kriging Interpolation. Air temperature raster layers were used as predictor variables in the spatial stream network models (SSNM).

Year	Thermal Metric	Minimum	Mean	Maximum
2019	Average Weekly Average Temperature	0.0024	0.96	2.26
2019	Maximum Weekly Average Temperature	0.0027	1.05	2.48
2019	Average Weekly Coefficient of Variation	0.045	17.69	41.62
2020	Average Weekly Average Temperature	0.0016	0.63	1.55
2020	Maximum Weekly Average Temperature	0.0012	0.48	1.18
2020	Average Weekly Coefficient of Variation	0.0380	14.65	35.76
2021	Average Weekly Average Temperature	0.0003	0.55	1.38
2021	Maximum Weekly Average Temperature	0.0007	1.27	3.21
2021	Average Weekly Coefficient of Variation	0.006	12.00	30.27

Table 2. Final spatial stream network models (SSNM) used in temperature predictions across the Parsnip River watershed. Model diagnostic statistics are presented along with model predictor and spatial covariance parameters.

Year	Thermal Response Metric	Predictor Variables	Spatial Covariance Parameters	Nugget Effect	R-Squared	RMSPE	Standardized Bias
2019	AWAT	Air AWAT + Reach Contributing Area	Epanech tailup, Exponential taildown, Cauchy Euclidean	No	0.050	0.472	0.009
2019	MWAT	Air MWAT + Reach Contributing Area	Mariah tailup, Mariah taildown, Gaussian Euclidean	No	0.087	0.511	0.009
2019	AWCV	Air AWCV	LinearSill tailup, Mariah taildown, Cauchy Euclidean	Yes	0.214	0.005	-0.0005
2020	AWAT	Air AWAT + Reach Contributing Area	Epanech tailup, Spherical taildown, Gaussian Euclidean	No	0.255	0.341	-0.013
2020	MWAT	Air MWAT + Reach Contributing Area	Exponential tailup, Mariah taildown, Gaussian Euclidean	Yes	0.295	0.681	-0.023
2020	AWCV	Air AWCV + Reach Contributing Area	Mariah tailup, Exponential taildown, Gaussian Euclidean	Yes	0.073	0.007	-0.0001
2021	AWAT	Air AWAT	Spherical Tailup, Epanech Taildown, Cauchy Euclidean	Yes	0.490	0.945	0.046
2021	MWAT	Air AWAT	Mariah Tailup, Exponential Taildown, Cauchy Euclidean	Yes	0.171	0.998	0.100
2021	AWCV	Air AWCV	LinearSill Tailup, Epanech Taildown, Spherical Euclidean	Yes	0.0003	0.008	0.005

Table 3. Model selection statistics for candidate SCR model models fitted to Arctic Grayling detection data.

Model	K	logLik	AICc	ΔAICc	wAICc
All trophic data (01 Jul - 15 Sep: All Years)					
D ~ Temp + BT	5	-12292.98	24596.40	0.00	0.99
D ~ BT + Year	6	-12296.09	24604.80	8.40	0.01
D ~ Temp + Year	6	-12325.19	24662.99	66.59	0.00
D ~ Temp + BT + Year	7	-12324.58	24663.98	67.58	0.00
D ~ BT	4	-12336.55	24681.39	84.99	0.00
Default (D, g0, σ ~ 1)	3	-12337.81	24681.79	85.38	0.00
D ~ Temp*Year + BT*Year	11	-19720.34	39464.69	14868.29	0.00
D ~ Temp	4	-24463.18	48934.65	24338.25	0.00
D ~ Temp*Year + BT	9	-24683.78	49386.91	24790.51	0.00
D ~ Temp + BT*Year	9	-24780.91	49581.17	24984.77	0.00
2019 Trophic period (01 July - 15 Sep 2019)					
D ~ Temp + BT	5	-4226.16	8463.49	0.00	1.00
D ~ BT	4	-4237.54	8483.85	20.36	0.00
D ~ Temp	4	-4243.20	8495.17	31.67	0.00
Default (D, g0, σ ~ 1)	3	-4253.33	8513.11	49.62	0.00
2020 Trophic period (01 July - 15 Sep 2020)					
D ~ Temp	4	-2506.92	5022.87	0.00	0.79
D ~ Temp + BT	5	-2507.22	5026.02	3.15	0.16
D ~ BT	4	-2509.71	5028.44	5.57	0.05
Default (D, g0, σ ~ 1)	3	-2841.78	5690.15	667.28	0.00
2021 Trophic period (01 July - 15 Sep 2021)					
D ~ BT	4	-1720.04	3449.13	0.00	0.42
Default (D, g0, σ ~ 1)	3	-1721.75	3450.13	1.00	0.26
D ~ Temp + BT	5	-1719.46	3450.54	1.41	0.21
D ~ Temp	4	-1721.37	3451.78	2.66	0.11

Notes: Covariates for temperature (Temp), density of the sampled Bull Trout population (BT), and Year are integrated as a state-space covariate on *D*. The first section (All trophic data) is fitted SCR models on aggregated data from the feeding window across all years. Year-specific models were fit below to assess the appropriate model to use creating the time series metrics. K: number of parameters in the model; logLik: model log likelihood; AICc: bias-corrected Akaike Information Criterion (model in a set with lowest value is the most parsimonious one to explain variability in the response variable); ΔAICc: difference in AICc between a model and the model with the lowest AICc; wAICc: weight AICc (interpreted as the probability that the model is the most parsimonious one among the models in the candidate set).

Table 4. Number of samples for stable isotope analysis collected throughout the study by watershed and sample type. Samples were collected from June to September 2018 to 2021.

Sample/Stream	Anzac	Hominka	Missinka	Table	Other	Total
Muscle	31	18	14	29	7	99
Adipose	52	40	22	80	16	210
Invertebrates	10	8	6	6	0	30
Prey Fish	15	9	4	11	2	41
Terrestrial Veg.	21	18	16	15	0	70
Periphyton	4	5	4	3	0	16
Total	133	98	66	144	25	466

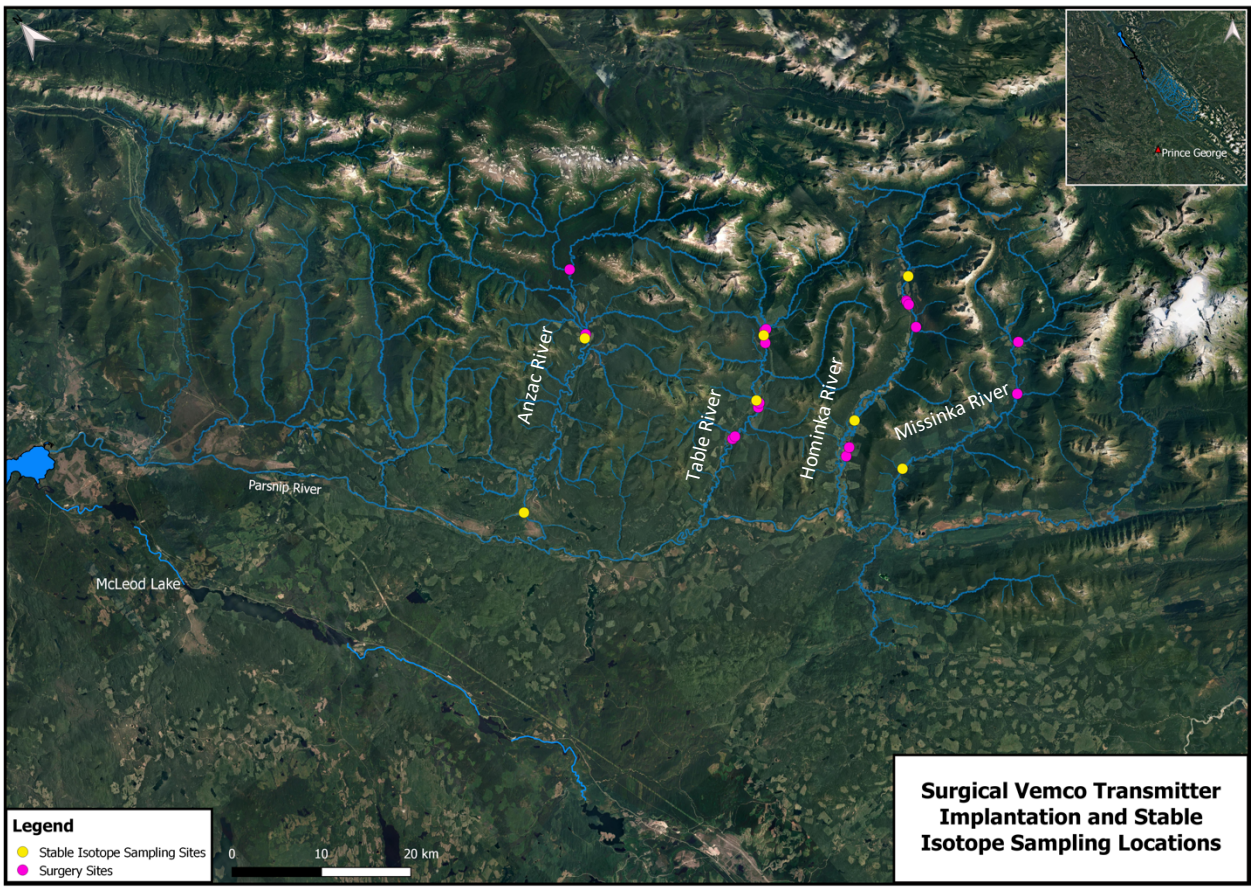

Figure 1. Locations of tag implantation surgery sites, and stable isotope sampling sites.

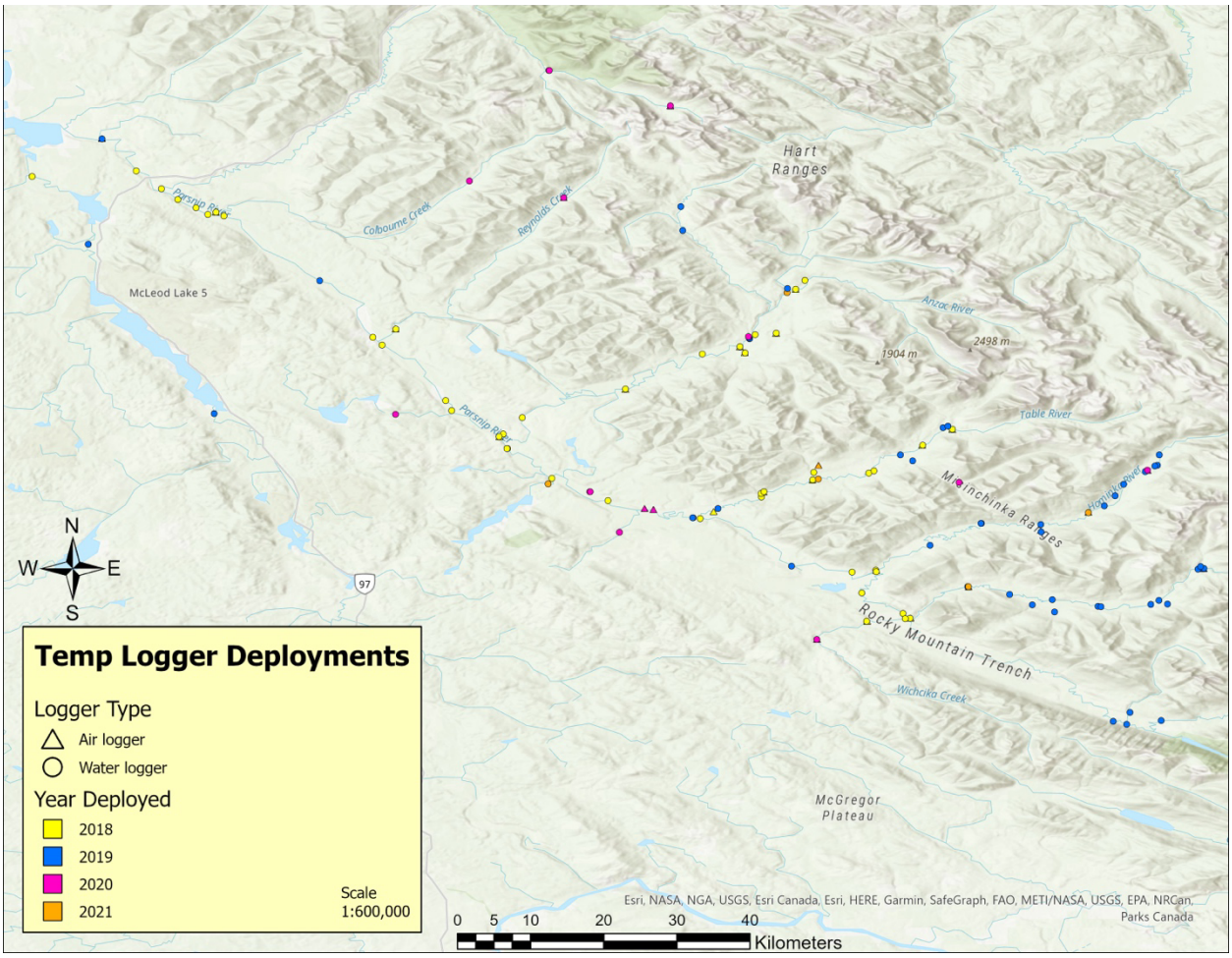

Figure 2. Locations of temperature data loggers deployed in the Parsnip River watershed.

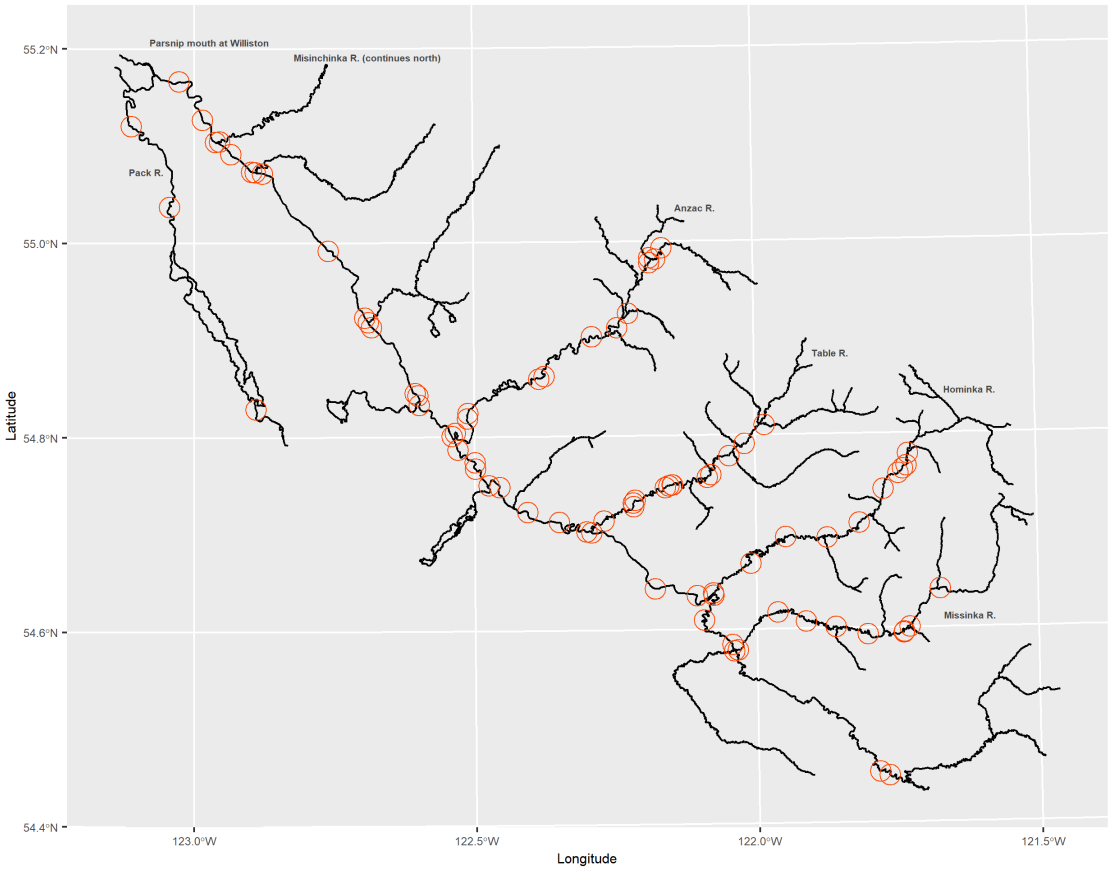

Figure 3. Spatial coverage of all acoustic receivers (red circles) deployed (including those that were eventually lost) during the study period (2018-2021).

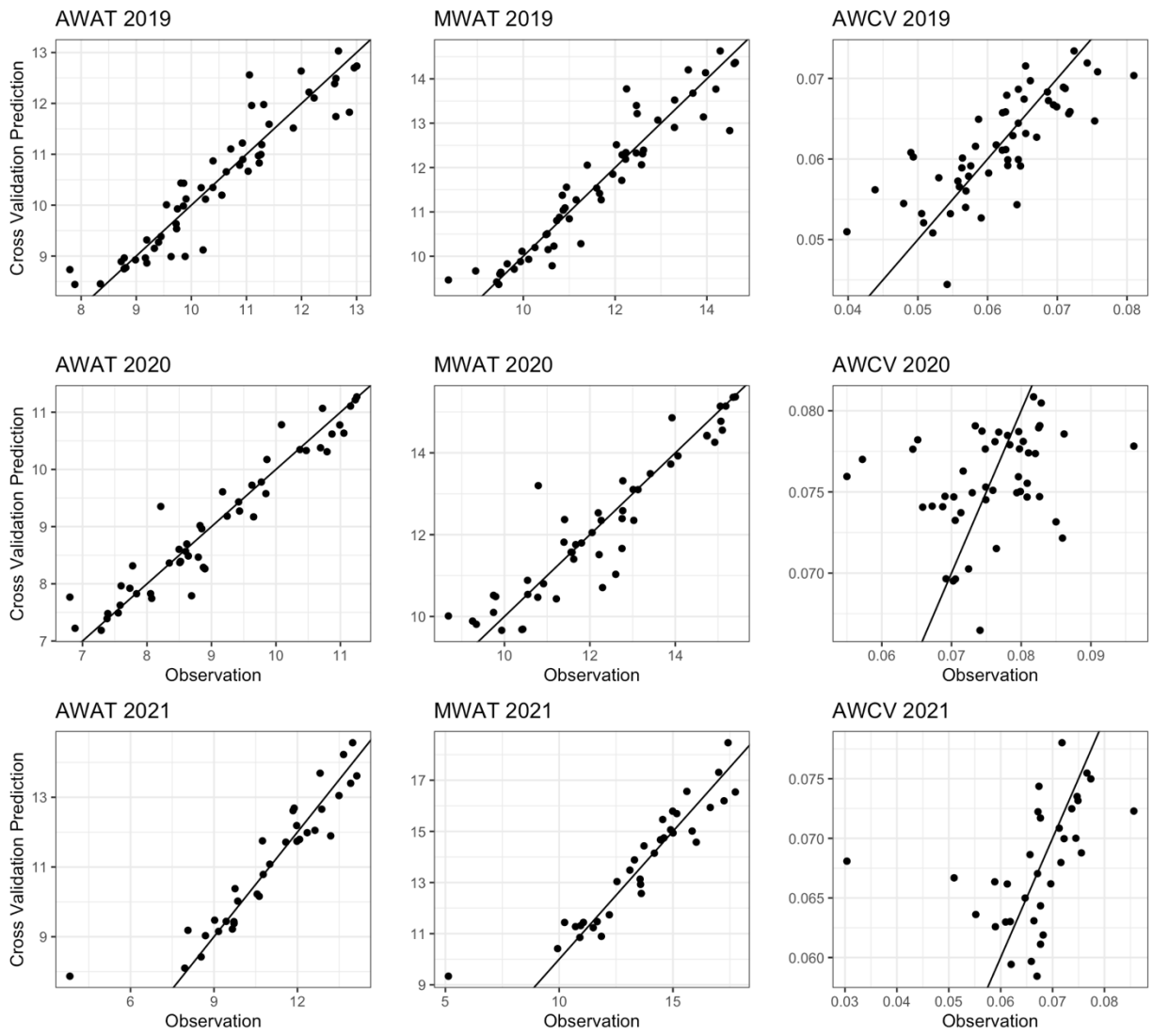

Figure 4. Leave-one-out cross validation predictions plotted against the observed data points for each spatial stream network model.

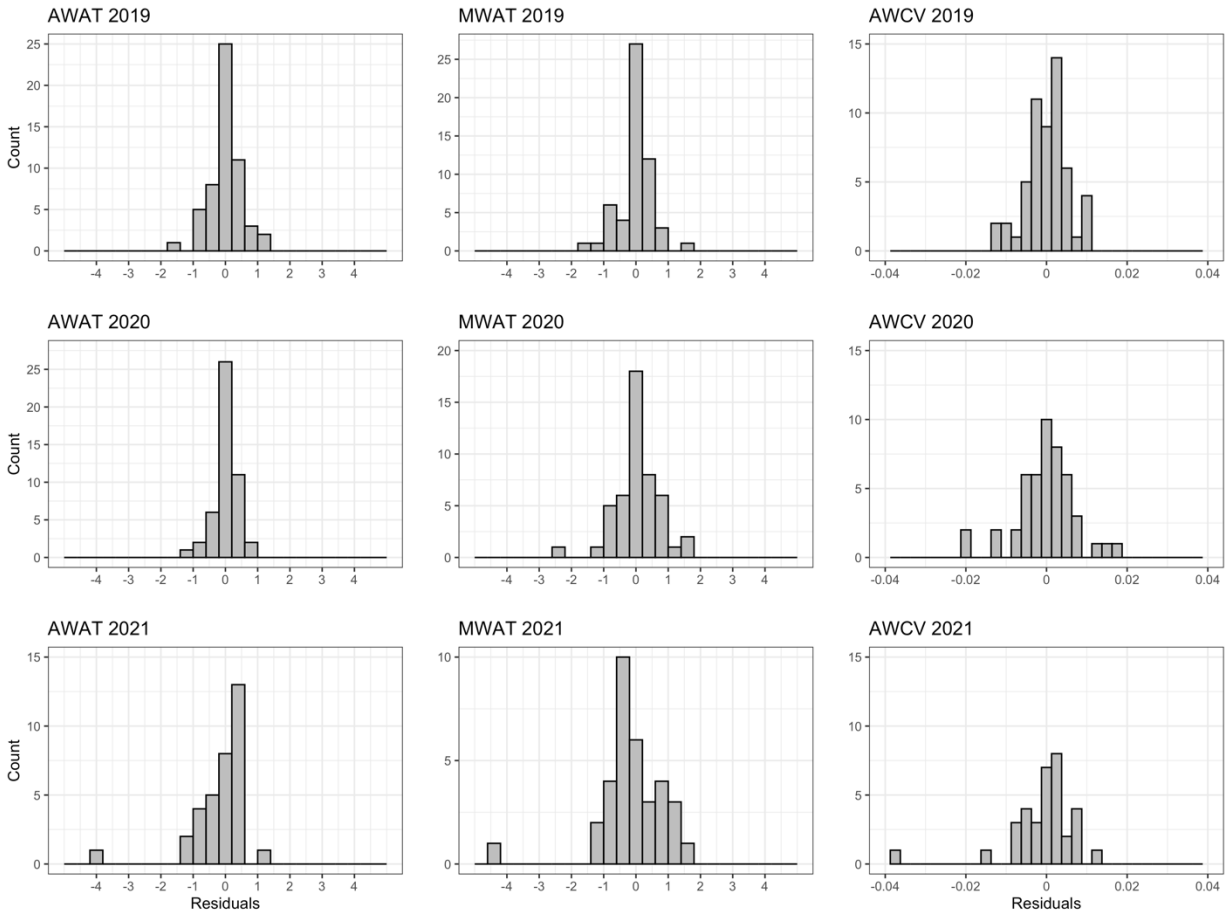

Figure 5. Histograms of leave-one-out cross validation residuals from fitted spatial stream network models.

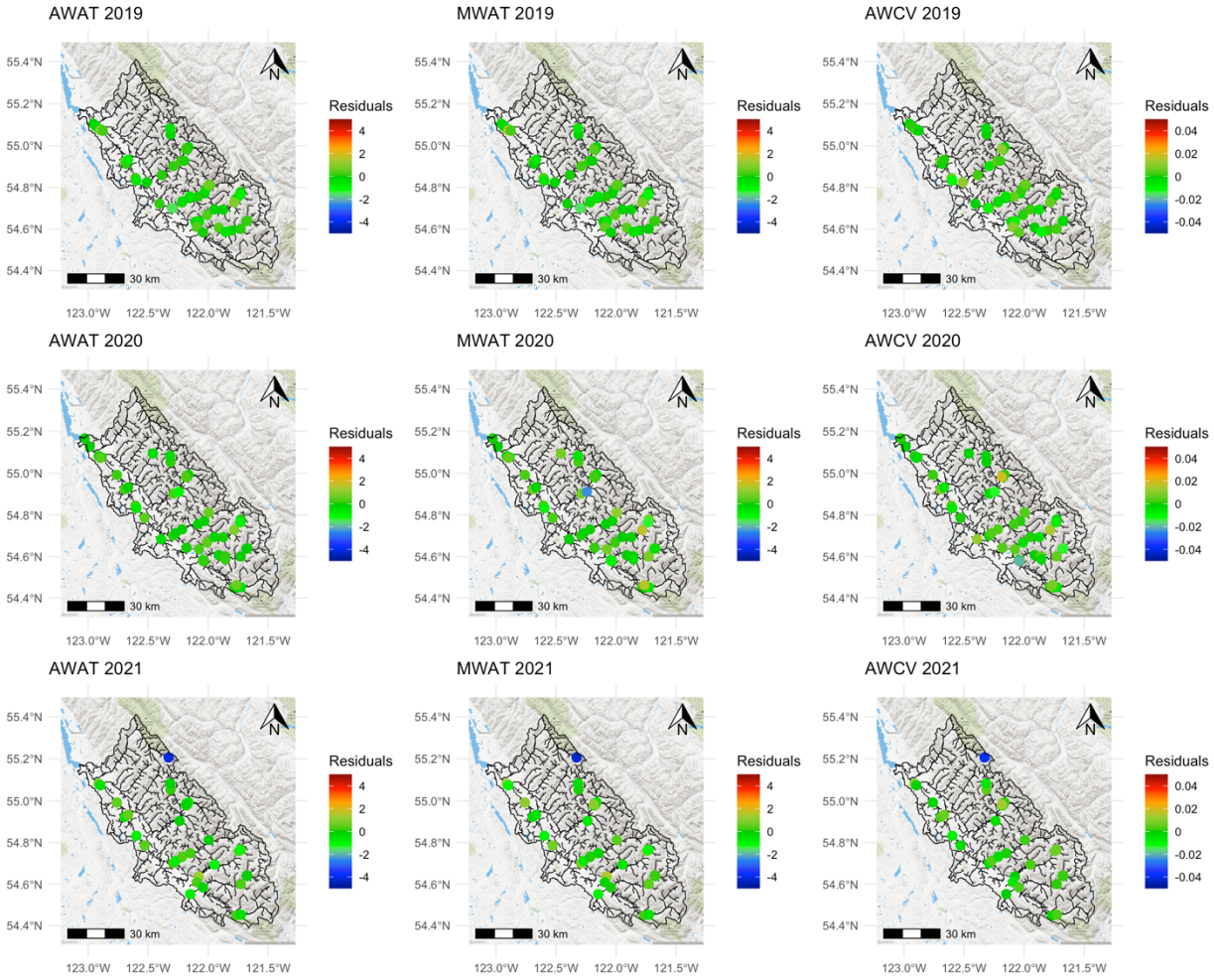

Figure 6. Spatial plots of leave-one-out cross validation residuals for average weekly average temperature (left) maximum weekly average temperature (middle) and average weekly coefficient of variation (right).

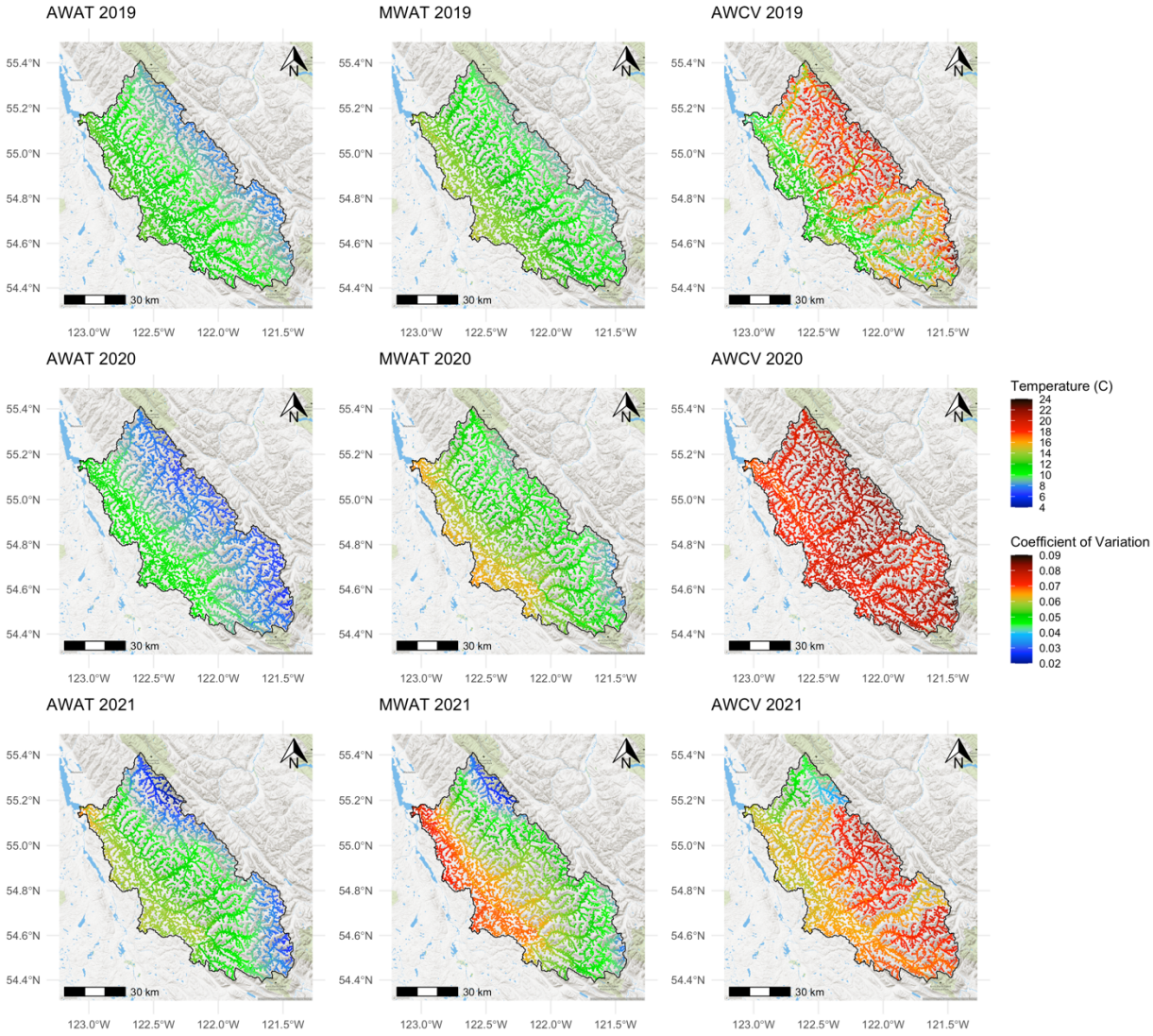

Figure 7. Average weekly average temperature (ºC; left), maximum weekly average temperature (ºC; middle) and average weekly coefficient of variation (right) spatial stream network model predictions for the Arctic frayling feeding window.

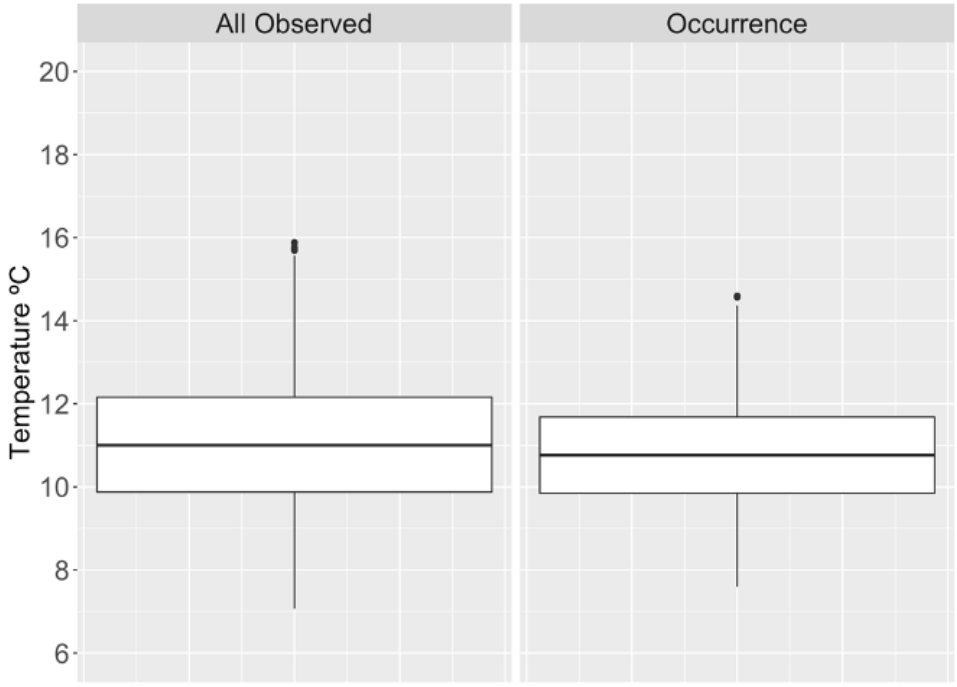

Figure 8. Box and whisker plot depicting observed 2019 daily average temperatures at all acoustic receiver sites (left) and at sites where Arctic Grayling were detected (right).

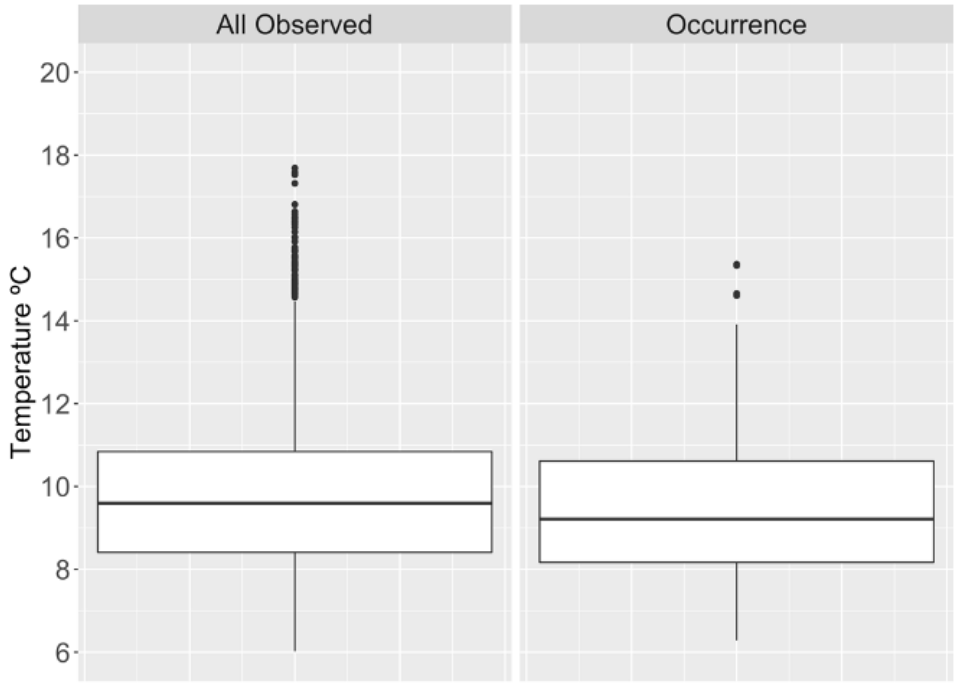

Figure 9. Box and whisker plot depicting observed 2020 daily average temperatures at all acoustic receiver sites (left) and at sites where Arctic Grayling were detected (right).

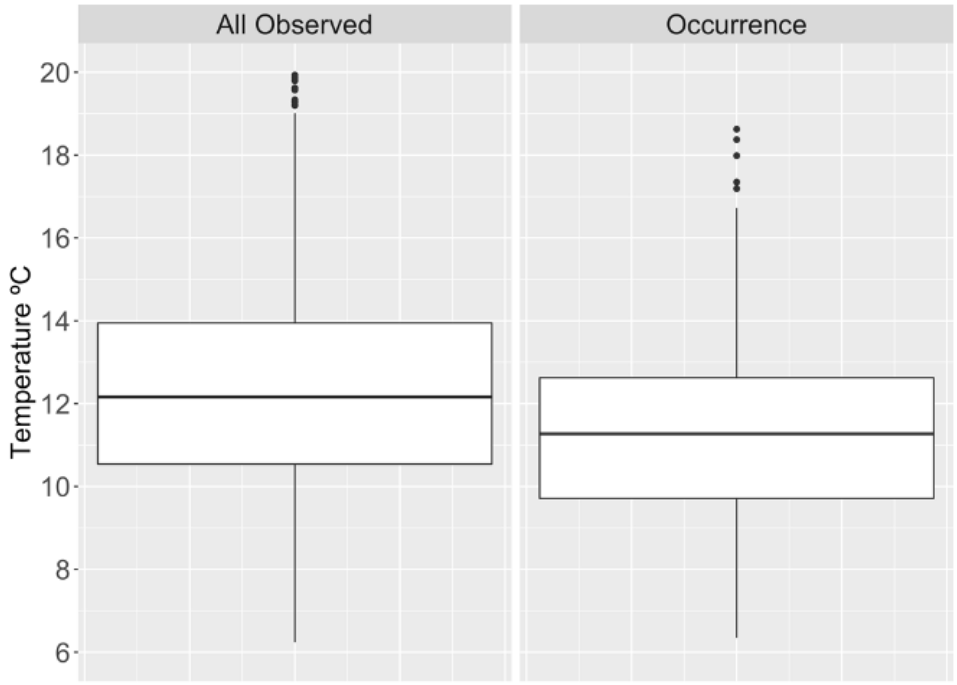

Figure 10. Box and whisker plot depicting observed 2021 daily average temperatures at all acoustic receiver sites (left) and at sites where Arctic Grayling were detected (right).

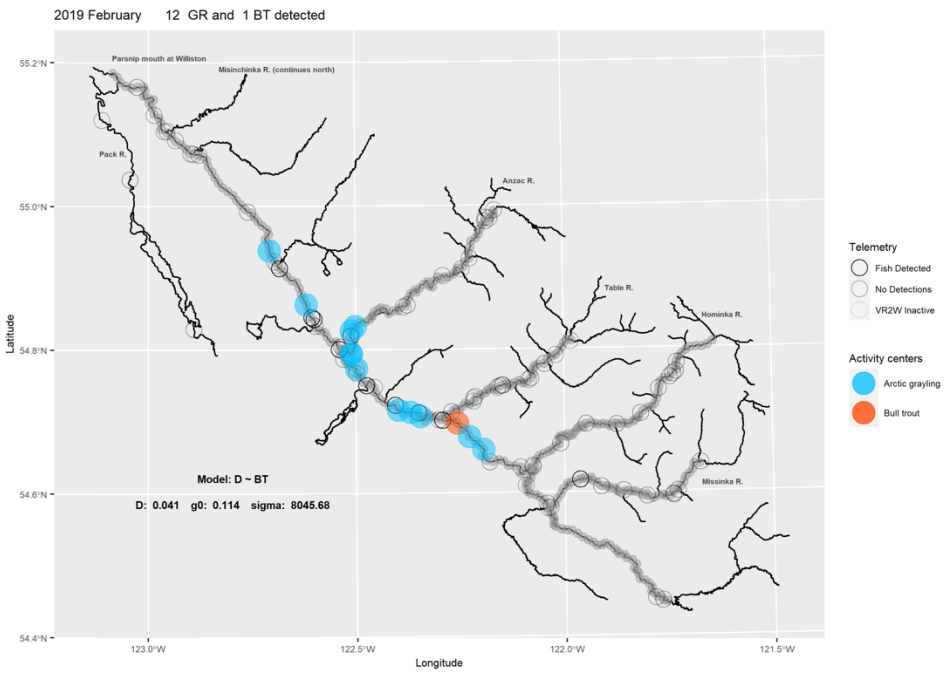

Figure 11. A representative SCR model output depicting a typical Arctic Grayling winter range

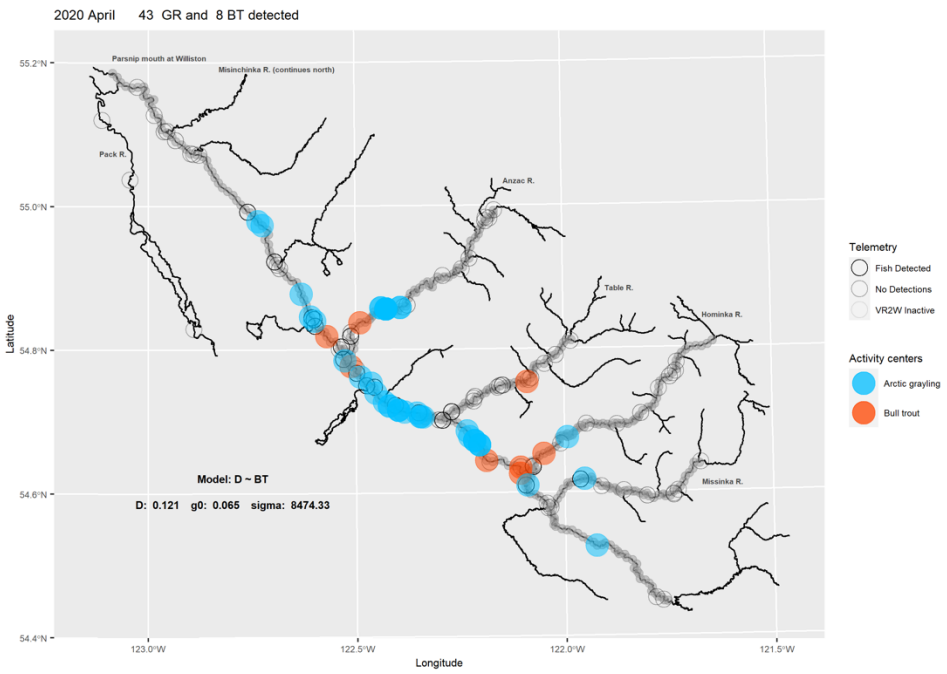

Figure 12. A representative SCR model output depicting a typical Arctic Grayling early springtime range.

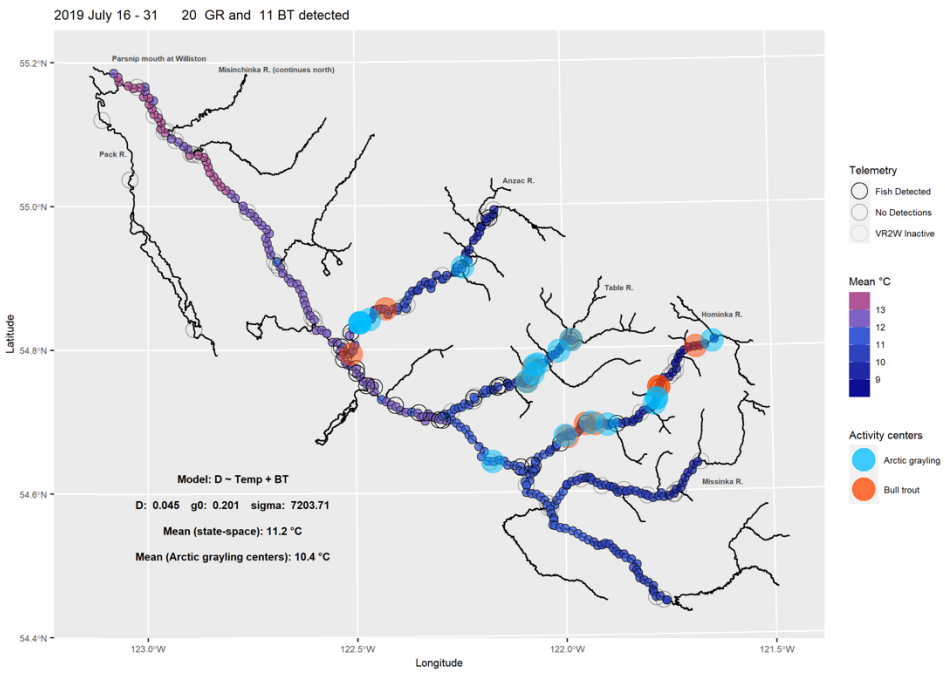

Figure 13. A representative SCR model output depicting a typical Arctic Grayling early summer range.

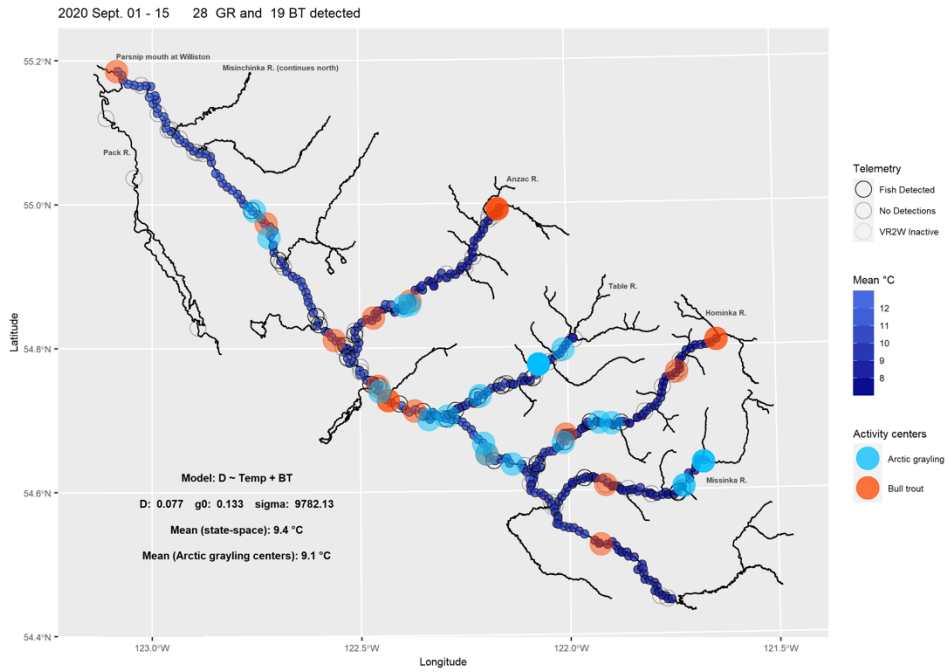

Figure 14. A representative SCR model output depicting a typical Arctic Grayling late summer/early fall range.

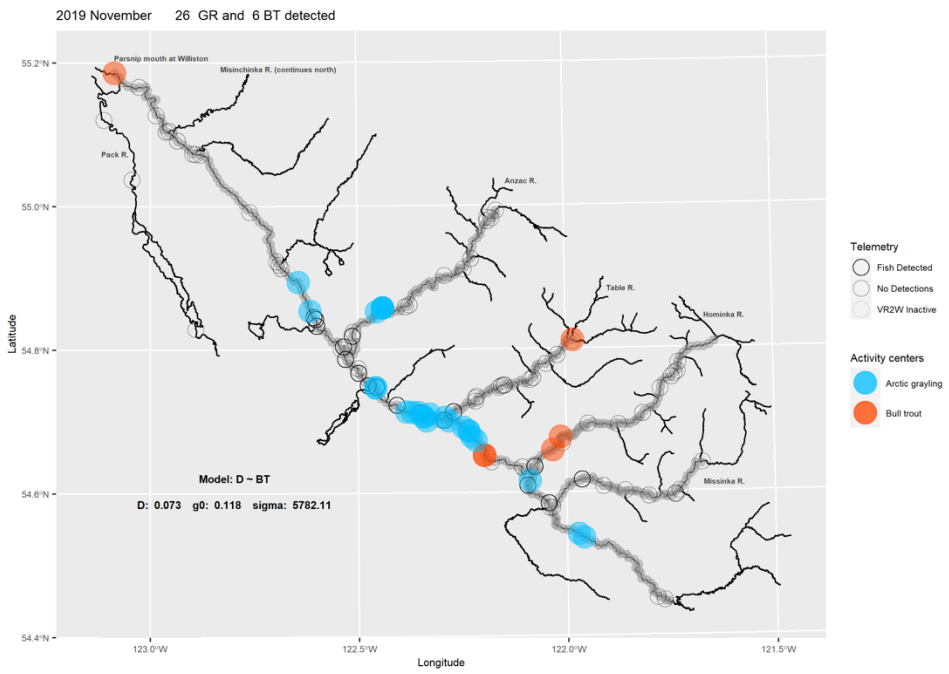

Figure 15. A representative SCR model output depicting a typical Arctic Grayling late fall/early winter range.

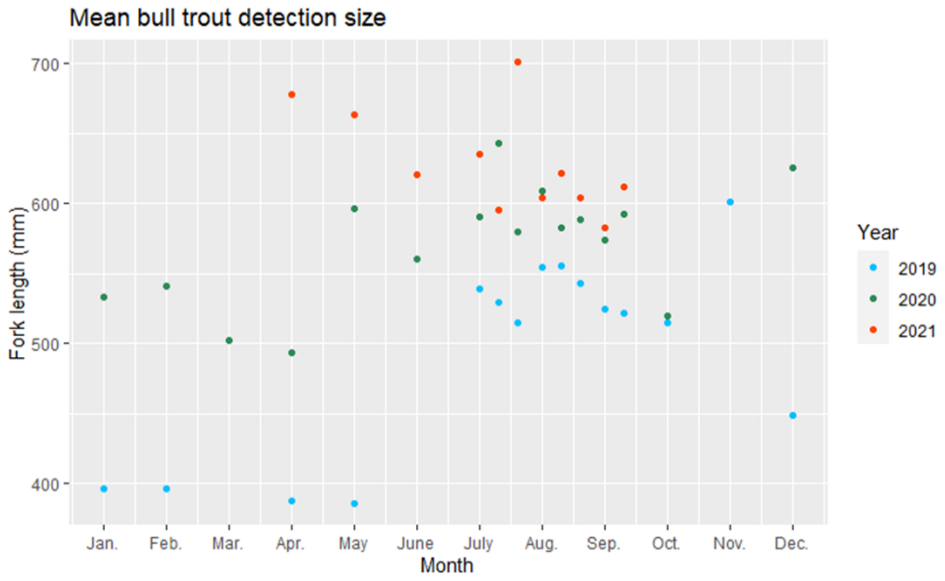

Figure 16. Mean fork lengths of Bull Trout detected within the Parsnip River watershed over time.

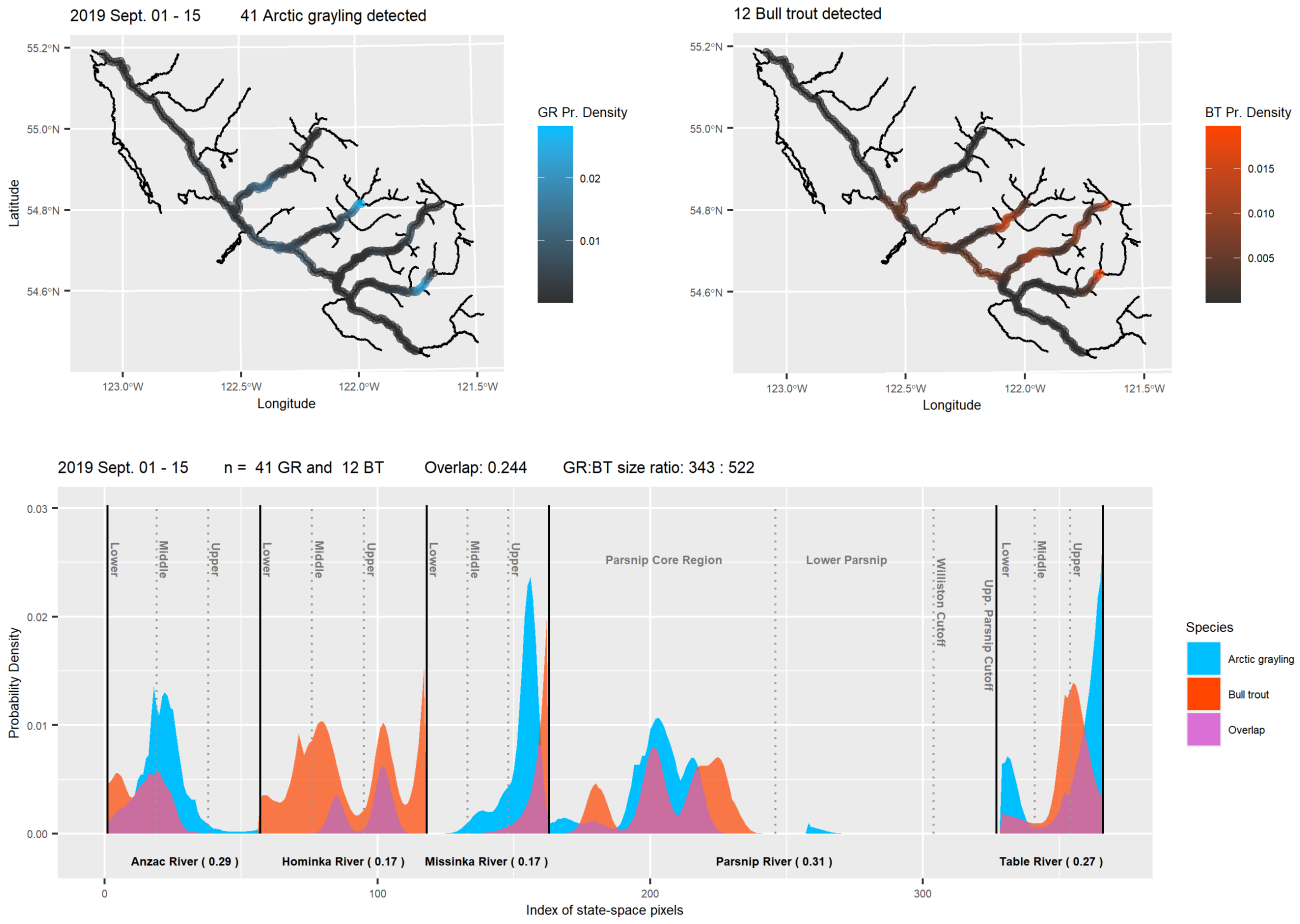

Figure 17. Results of an overlap analysis for the 2019 early September feeding window. Heavy lines mark the mouths and distal extents of each River. Light lines represent low, mid, and upper reaches of each tributary. The Parsnip is broken into the Parsnip core r core region (the mainstem between the four study tributaries plus an extend reach downstream of the Anzac), the lower Parsnip, and a small subsection of pixels represents the upper Parsnip. A full description of overlap interpretation can be found in Appendix A.

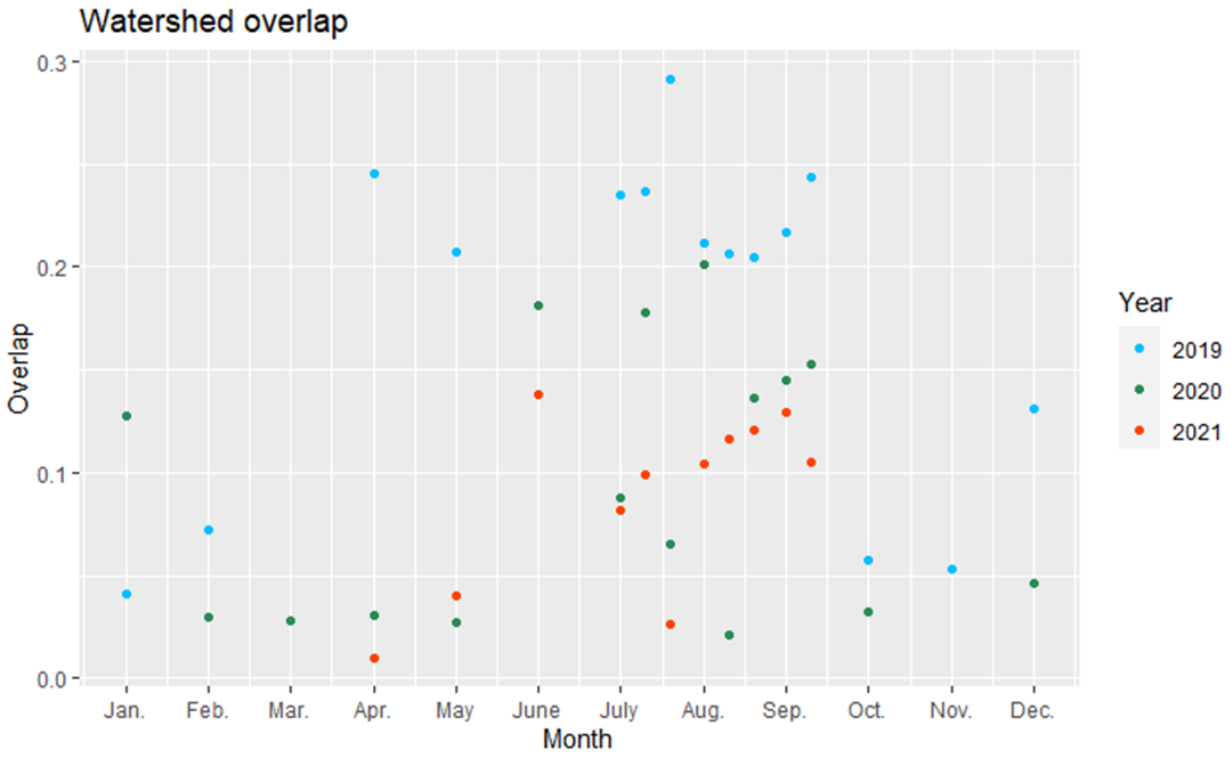

Figure 18. Watershed-level spatial overlap between Arctic Grayling and Bull Trout over time.

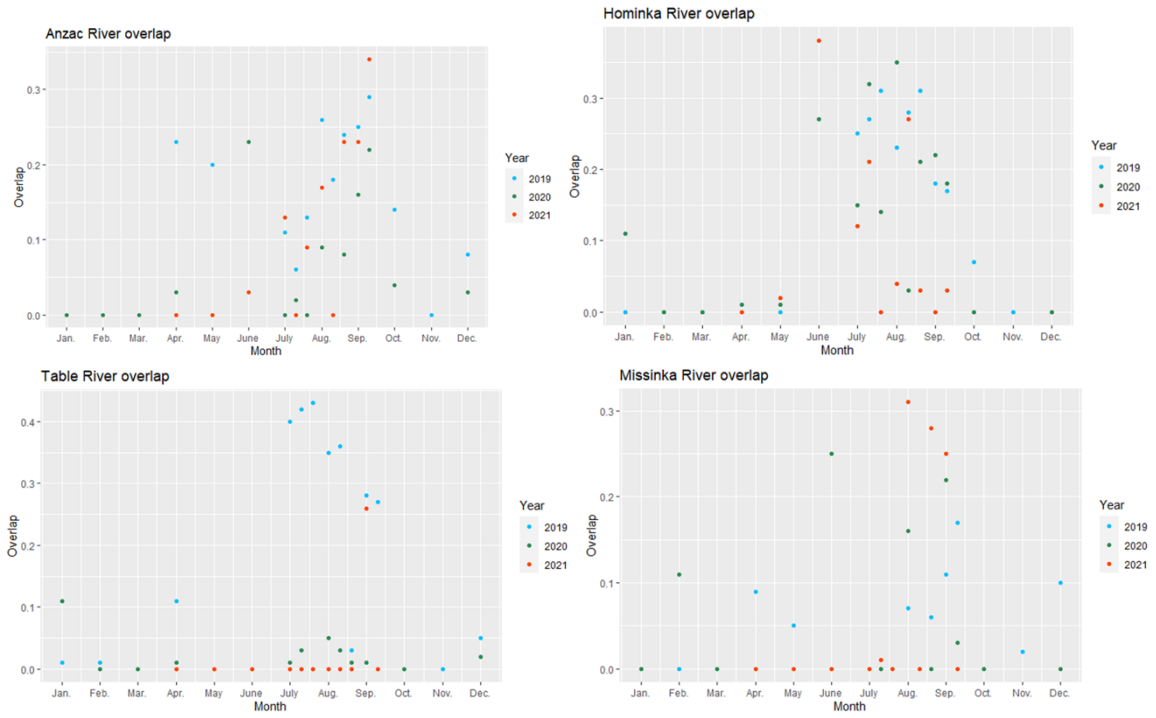

Figure 19. Tributary-level spatial overlap between Arctic Grayling and Bull Trout over time.

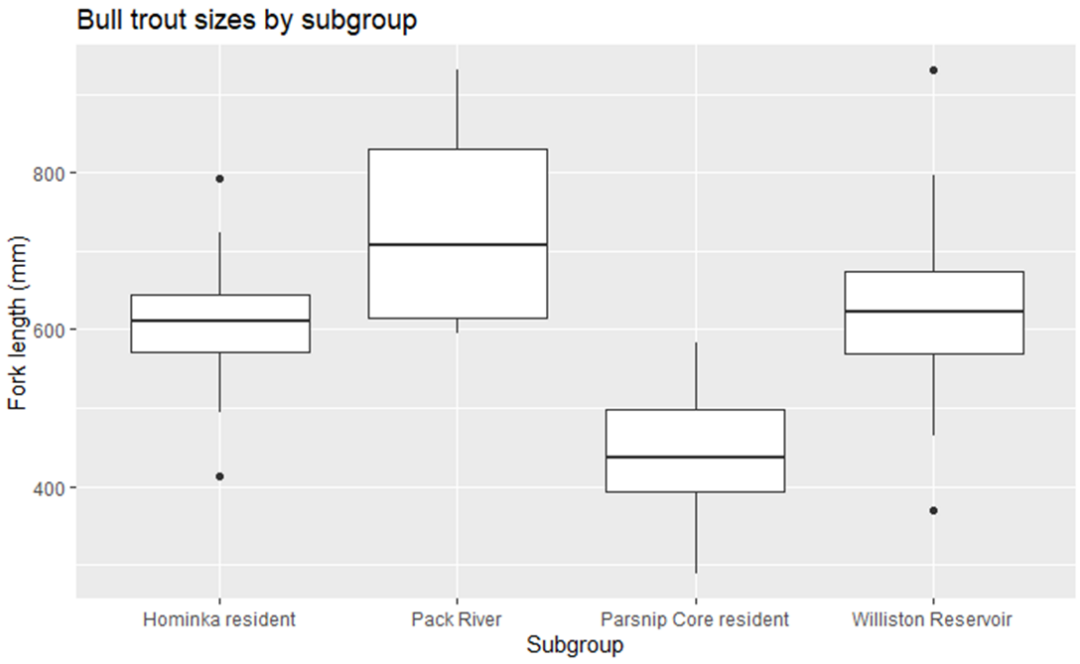

Figure 20. Fork length means of sampled Bull Trout grouped by apparent area use.

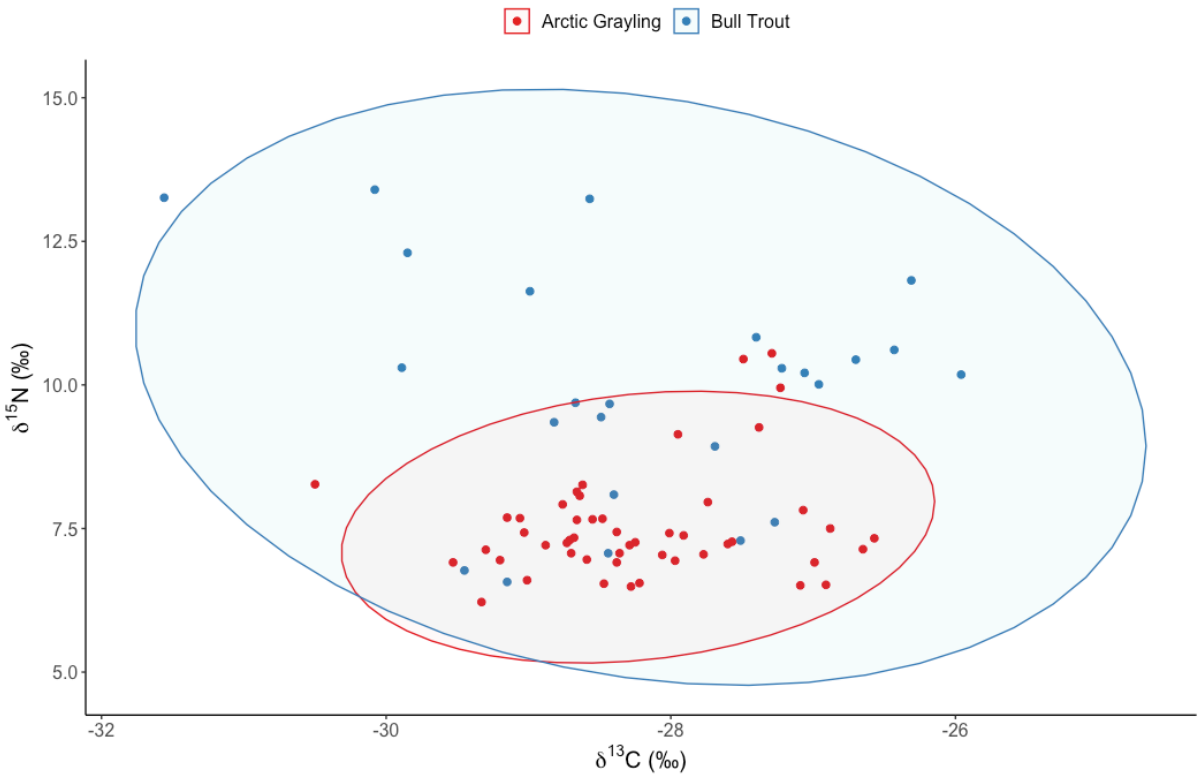

Figure 21. Isotope biplot fitted with 95% ellipses quantifying summer isotopic niche occupied by both Arctic Grayling and Bull Trout within the Parsnip River watershed. Isotopic signatures were derived from muscle tissue collected between 2018 and 2021.

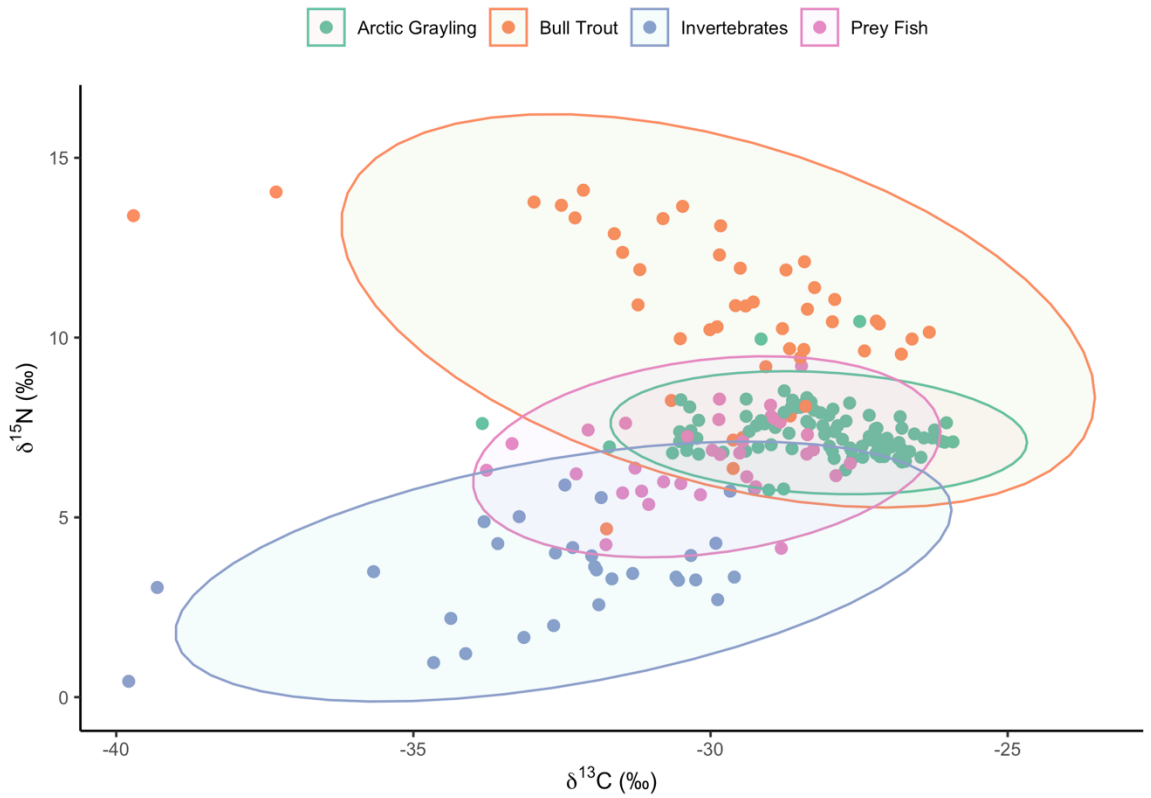

Figure 22. Isotope biplot fitted with 95% ellipses quantifying summer isotopic niche area occupied Arctic Grayling, Bull Trout, prey fish and aquatic invertebrates within the Parsnip system. Isotopic signatures were derived from muscle samples or whole organism (prey fish, invertebrates) collected between 2018 and 2021.

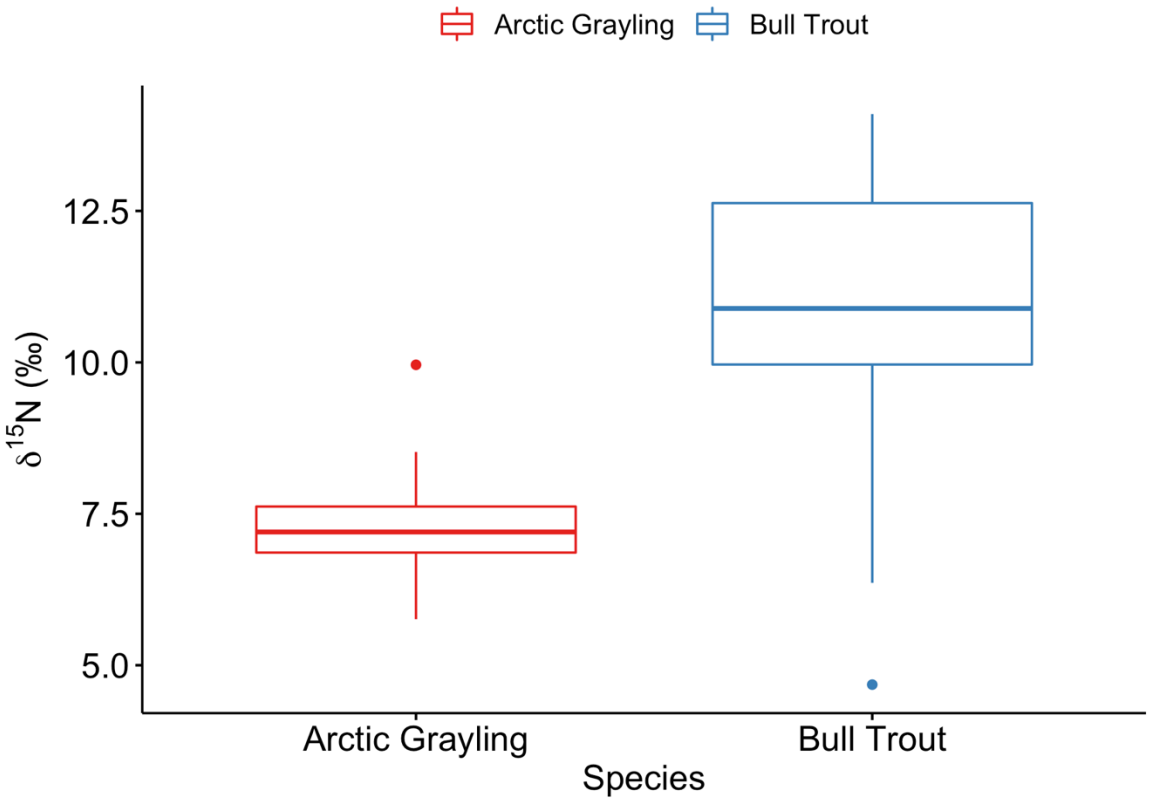

Figure 23. Box and whisker plot depicting the distribution of $\delta^{15}N$ values from sampled Arctic Grayling and Bull Trout in the Parsnip River watershed.

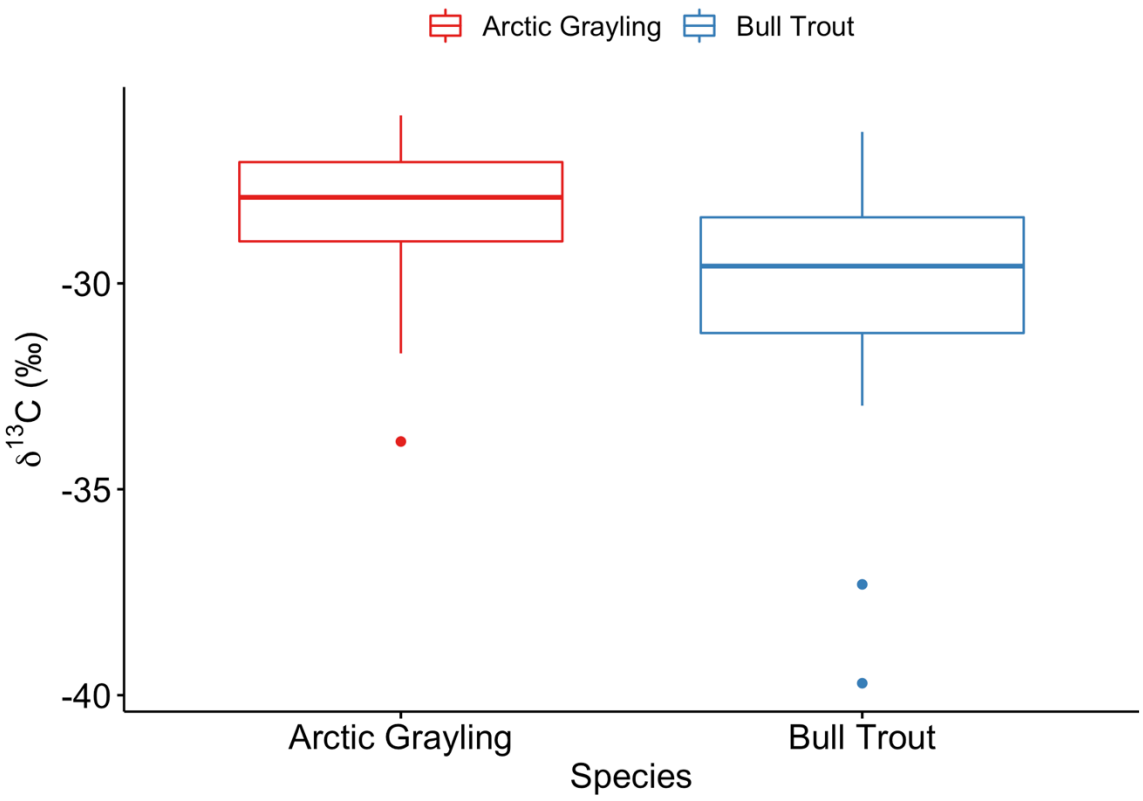

Figure 24. Box and whisker plot depicting the distribution of δ13C values from sampled Arctic Grayling and Bull Trout in the Parsnip River watershed.

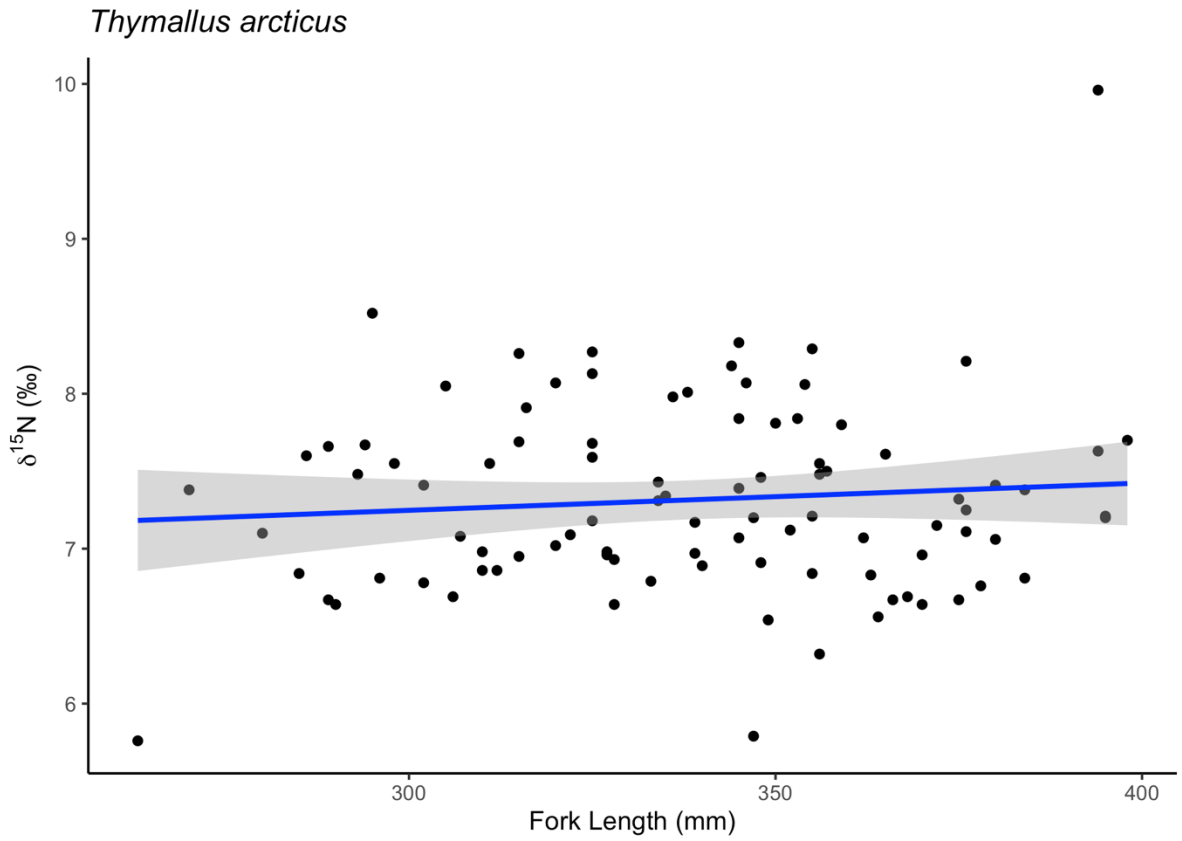

Figure 25. $\delta^{15}N$ in muscle tissue as a function of fork length in Arctic Grayling. Muscle samples were collected in the Parsnip watershed during the summers of 2018-2021 ($y = 4.68x + 304.10$, $R^2 = 0.008$, $P = 0.38$).

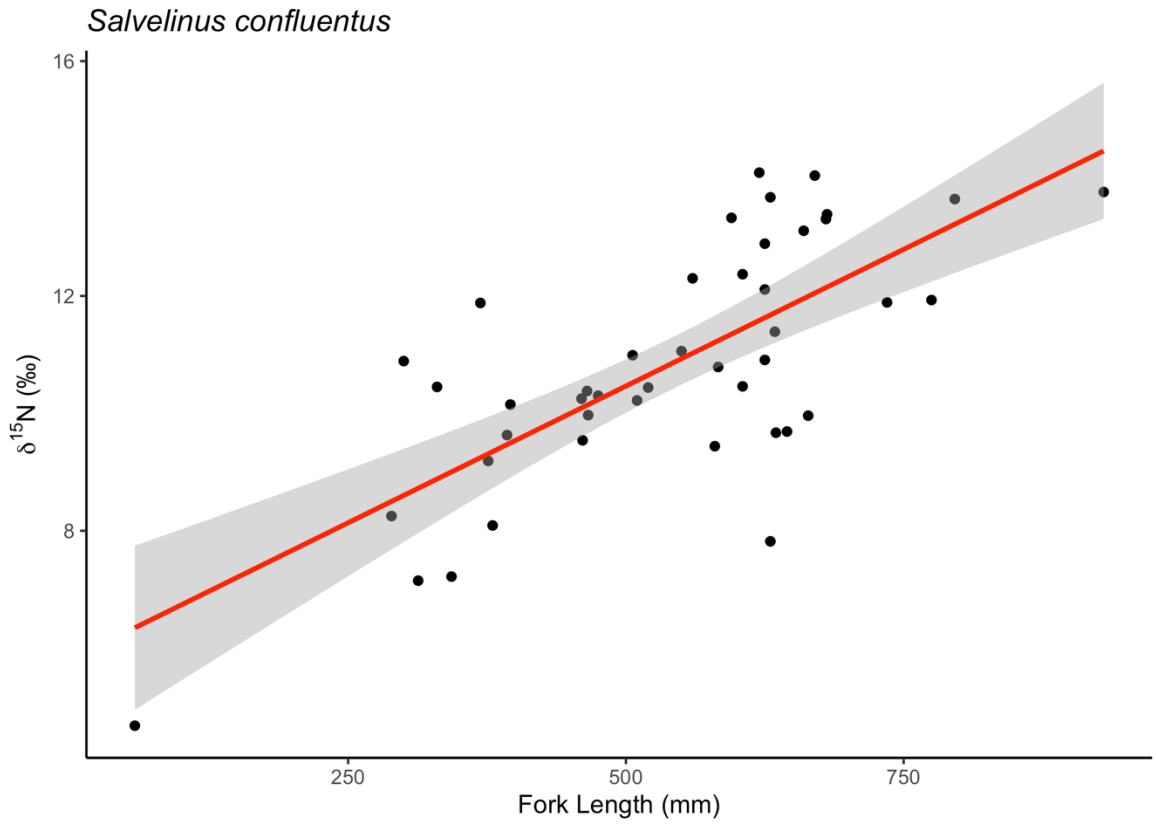

Figure 26. $\delta^{15}N$ in muscle tissue as a function of fork length in Bull Trout. Muscle samples were collected in the Parsnip watershed during the summers of 2018-2021 ($y = 0.0093x + 5.81$, $R^2 = 0.51$, $P < 0.001$).